



UNIVERSIDADE D
COIMBRA

Viviane Setti Barroso

A CONSISTENT LINEAR TWO-DIMENSIONAL
MATHEMATICAL MODEL FOR THIN TWO-LAYER
PLATES WITH PARTIAL SHEAR INTERACTION

Dissertation submitted in partial fulfilment of the requirements for the degree of Master in Civil Engineering, area of expertise in Structures, supervised by Professor Anísio Andrade and Professor Paulo Providência e Costa and presented to the Civil Engineering Department of the Faculty of Sciences and Technology of University of Coimbra.

October 2020

Faculty of Sciences and Technology of the University of Coimbra
Department of Civil Engineering

Viviane Setti Barroso

A CONSISTENT LINEAR TWO- DIMENSIONAL MATHEMATICAL MODEL FOR THIN TWO-LAYER PLATES WITH PARTIAL SHEAR INTERACTION

UM MODELO MATEMÁTICO BIDIMENSIONAL LINEAR PARA PLACAS
FINAS DE DUAS CAMADAS COM INTERACÇÃO DE CORTE PARCIAL

Dissertation submitted in partial fulfilment of the requirements for the degree of
Master in Civil Engineering, area of expertise in Structures, supervised by Prof.
Anísio Andrade and Prof. Paulo Providência e Costa

This dissertation is the sole responsibility of the author. The Department of Civil Engineering of the Faculty of Sciences and
Technology of the University of Coimbra declines any responsibility, legal or otherwise, in relation to errors or omissions that it
may contain.

October 2020



UNIVERSIDADE DE
COIMBRA

ACKNOWLEDGEMENTS

I wish to express my special gratitude to Professor Doctor Anísio Alberto Martinho de Andrade and Professor Doctor Paulo Manuel Mendes Pinheiro da Providência e Costa for their able guidance and support during this dissertation and during my bachelor's and master's degrees in civil engineering.

To all my teachers until now, I would like to thank you for all the knowledge and inspiration you gave me, thus making it possible for me to flourish.

To my family, I am deeply grateful for the support and encouragement during my academic life. You are both my anchor that holds me through life's storms and the guiding hand that make it possible for me to reach new heights.

To my friends, I am grateful for your support and encouragement during this phase.

“If I have seen further it is by standing on the shoulders of Giants” – Isaac Newton.

Thank You!

Viviane Setti Barroso

ABSTRACT

This dissertation presents a consistent derivation, from three-dimensional linear elasticity, of a two-dimensional mathematical model describing the bending and in-plane stretching behaviours, under a general system of quasi-static distributed loads and prescribed support displacements, of thin two-layer plates with partial shear interaction. The following key assumptions are made:

- (i) Each layer, when considered separately, behaves as a Kirchhoff plate.
- (ii) The interlayer (with non-zero thickness), when considered separately, behaves as a transverse shear-only Mindlin plate.
- (iii) Each layer is bonded to the interlayer in such a way that both sliding and detachment are prevented.

The dimensional reduction stage of the derivation, from three spatial dimensions to just two, is accomplished by means of Podio-Guidugli's method of internal constraints. This is followed by a process of assembly or aggregation, in which the continuity of displacements and certain stress components across each layer/interlayer interface is enforced.

A problem with closed-form analytical solution illustrates the application of the two-dimensional model and its capabilities. In particular, the solution is proven to be continuous across the whole range of zero, partial and full interaction between the layers. The problem is then generalized and a Navier-type solution is obtained. The results are compared with those reported in the literature.

Possible applications of the model include the analysis of laminated glass plates under quasi-static short-term loads in service conditions and within a limited temperature range.

Keywords: Thin two-layer plates, partial shear interaction, linear two-dimensional mathematical model, internal constraints, laminated glass

RESUMO

Nesta dissertação apresenta-se uma dedução consistente, a partir da teoria da elasticidade linear tridimensional, de um modelo matemático bidimensional que descreve o comportamento à flexão e no plano, sob um sistema geral de cargas distribuídas quase-estáticas e deslocamentos impostos nos apoios (“assentamentos”), de placas finas de duas camadas com interação de corte parcial. Admitem-se as seguintes hipóteses fundamentais:

- (i) Cada camada, quando considerada isoladamente, comporta-se como uma placa de Kirchhoff.
- (ii) A intercamada (com espessura não nula), quando considerada isoladamente, comporta-se como uma placa de Mindlin e apresenta apenas resistência ao corte transversal.
- (iii) A ligação entre cada camada e a intercamada é perfeita, considerando-se assim impedidos tanto o deslizamento como o afastamento nessas superfícies de descontinuidade material.

A etapa de redução do número de dimensões espaciais de três para duas é realizada por intermédio do método de restrições internas proposto por Podio-Guidugli. Segue-se um processo de agregação, no qual se impõe, em cada interface camada/intercamada, a continuidade dos deslocamentos e de certas componentes de tensão.

Um problema com a solução analítica ilustra as potencialidades do modelo desenvolvido. Em particular, mostra-se que a solução é contínua em toda a gama de interação entre camadas, desde a interação nula até à interação total. Este problema é depois generalizado e obtém-se uma solução do tipo Navier. Os resultados são comparados com os disponíveis na literatura.

De entre as possíveis aplicações do modelo, destaca-se a análise de placas de vidro laminado sob a acção de cargas quase-estáticas de curta duração, em condições de serviço e dentro de uma gama de temperaturas limitada.

Palavras-chave: Placas finas de duas camadas, interacção de corte parcial, modelo matemático bidimensional linear, restrições internas, vidro laminado

CONTENTS

1 INTRODUCTION.....	1
1.1 Laminated glass and its mechanical behaviour	1
1.2 Objective and scope of the dissertation	3
1.3 Outline of the dissertation.....	5
2 TWO-DIMENSIONAL MATHEMATICAL MODEL	7
2.1 Preliminary considerations	7
2.2 Assumptions	9
2.3 Kinematics	10
2.4 Constitutive equations	17
2.5 Equilibrium	21
2.6 The boundary value problem for the top-tier generalized displacements.....	29
3 AN ILLUSTRATIVE PROBLEM WITH CLOSED-FORM EXACT SOLUTION AND ITS GENERALIZATION ...	32
4 SUMMARY AND CONCLUSIONS. RECOMMENDATIONS FOR FUTURE WORK	47
APPENDIX 1: A SUMMARY, IN THE FORM OF A TONTI DIAGRAM, OF THE TOP-TIER FIELD EQUATIONS OF THE TWO-DIMENSIONAL MODEL.....	49
APPENDIX 2: THE REACTIVE STRESS FIELDS $\tau_{xz,i}$, $\tau_{yz,i}$ AND $\sigma_{z,i}$ ON EACH LAYER; THE REACTIVE STRESS FIELD $\sigma_{z,s}$ ON THE INTERLAYER	54
REFERENCES.....	60

LIST OF FIGURES

Figure 1.1: Apple Store – 5th Avenue, New York, 2011	1
Figure 1.2: Glass bridge with a 21 m span – Champalimaud Centre for the Unknown, Lisbon, 2010	2
Figure 2.1: Two-layer plate – Cartesian coordinate system and reference configuration.....	8
Figure 2.2: Displacement field	13
Figure 2.3: Surface tractions on the end faces and body forces for each of the two layers and for the interlayer.....	22
Figure 2.4: Through-the-thickness stress resultants on each layer and on the interlayer.....	24
Figure 3.1: Illustrative problem – Geometry, loading and boundary conditions	32
Figure 3.2: Illustrative problem – Qualitative shape of the distributions of “Kirchhoff” and “Mindlin” bending moments, assuming $q_0 > 0$ and $\nu > \max \left\{ -\left(\frac{a}{b}\right)^2, -\left(\frac{b}{a}\right)^2 \right\}$	36
Figure 3.3: Illustrative problem – Qualitative shape of the distributions of “Kirchhoff” and “Mindlin” twisting moments, assuming $q_0 > 0$	36
Figure 3.4: Illustrative problem – Qualitative shape of the distribution of “Mindlin” shear forces Q_x^M , assuming $q_0 > 0$	37
Figure 3.5: Illustrative problem – Qualitative shape of the distribution of “Mindlin” shear forces Q_y^M , assuming $q_0 > 0$	37
Figure 3.6: Illustrative example – Determination of the vertical support reactions.....	40
Figure 3.7: Illustrative problem – Vertical support reactions	40

Figure 3.8: Truncated Fourier sine series expansion of a uniform load q_0 on the interior of the rectangle $[0, a] \times [0, b]$	43
Figure A1.1: Tonti diagram of structural relations	53
Figure A2.1: Through-the-thickness distribution of shear stresses $\tau_{xz,i}$ ($i = 1, 2$), assuming that the body forces $b_{x,i}$ are independent of z	57

LIST OF TABLES

Table 3.1: Case studies – Maximum deflections.....	45
Table 3.2: Case studies – Maximum transverse shear strains in the interlayer.....	46

LIST OF SYMBOLS

Latin letters

a, b – rectangular plate dimensions

$b_{x,i}, b_{y,i}, b_{z,i}$ – Cartesian components of the body forces per unit volume acting in layer i

\mathbf{d} – column vector of upper-tier generalized displacements

E_i – Young modulus in the isotropy plane for the material of layer i

$G_{z,s}$ – shear modulus of the interlayer for shear stresses parallel to the direction of monotropy

h_i – thickness of layer i

h_s – thickness of the interlayer

\mathbf{k} – stiffness matrix

$\mathbf{k}_{m,i}$ – membrane stiffness matrix of each layer i

$\mathbf{k}_{b,i}$ – bending stiffness matrix of each layer i

\mathbf{L} – kinematics operator (formal linear differential operator)

\mathbf{L}^\dagger – equilibrium operator (formal adjoint of \mathbf{L})

$m_{x,i}, m_{y,i}$ – Cartesian components of the resultant moment distribution, with respect to the plane $z = z_i$, on layer i , defined per unit area of Ω

$m_{x,s}, m_{y,s}$ – Cartesian components of the resultant moment distribution, with respect to the plane $z = z_s$, on the interlayer, defined per unit area of Ω

$\mathbf{M}^K, \mathbf{M}^M$ – subvector of Kirchhoff” and “Mindlin” bending and twisting moments (upper-tier generalized stresses)

-
- $M_{x,i}, M_{y,i}, M_{xy,i}$ – bending and twisting moments in layer i (intermediate-tier generalized stresses)
- M_x^K, M_y^K, M_{xy}^K – “Kirchhoff” bending and twisting moments (upper-tier generalized stresses)
- M_x^M, M_y^M, M_{xy}^M – “Mindlin” bending and twisting moments (upper-tier generalized stresses)
- $\mathbf{n} = (n_x, n_y)$ – unit outer normal vector along the boundary Γ of Ω
- \mathbf{N} – subvector of membrane forces (upper-tier generalized stresses)
- N_x, N_y, N_{xy} – membrane forces (upper-tier generalized stresses)
- $N_{x,i}, N_{y,i}, N_{xy,i}$ – membrane forces in layer i (intermediate-tier generalized stresses)
- \mathbf{q} – column vector of plate loads (corresponding to the generalized displacements)
- q_0 – reference load
- $q_{m \cdot n}$ – Fourier coefficients of a uniform load q_0 on the interior of the rectangle $[0, a] \times [0, b]$
- $q_x, q_y, q_z, m_x^K, m_y^K, m_x^M, m_y^M$ – plate loads
- $q_{x,i}, q_{y,i}, q_{z,i}$ – Cartesian components of the resultant force distribution on layer i , defined per unit area of Ω
- $q_{z,s}$ – component in the z -direction of the resultant force distribution on the interlayer, defined per unit area of Ω
- \mathbf{Q}^M – subvector of “Mindlin” transverse shear forces (upper-tier generalized stresses)
- $Q_{x,i}, Q_{y,i}$ – transverse shear forces in layer i (intermediate-tier generalized stresses)
- Q_x^M, Q_y^M – “Mindlin” transverse shear forces (upper-tier generalized stresses)
- $Q_{x,s}, Q_{y,s}$ – transverse shear forces in the interlayer (intermediate-tier generalized stresses)
- Q_x, Q_y – total transverse shear forces in the layered plate (upper-tier generalized stresses)
- $r(x, y)$ – distributed vertical reactions along an edge
- R_0 – corner reactions
-

$s_{x,i}^-, s_{y,i}^-, s_{z,i}^-$ – Cartesian components of the surface tractions per unit area on the “top” face $\bar{\Omega} \times \{z_i - \frac{1}{2}h_i\}$ of layer i

$s_{x,i}^+, s_{y,i}^+, s_{z,i}^+$ – Cartesian components of the surface tractions per unit area on the “bottom” face $\bar{\Omega} \times \{z_i + \frac{1}{2}h_i\}$ of layer i

$s_{x,s}^-, s_{y,s}^-, s_{z,s}^-$ – surface tractions acting on “top” face $\bar{\Omega} \times \{z_s - \frac{1}{2}h_s\}$ of the interlayer

$s_{x,s}^+, s_{y,s}^+, s_{z,s}^+$ – surface tractions acting on “bottom” face $\bar{\Omega} \times \{z_s + \frac{1}{2}h_s\}$ of the interlayer

$\mathbf{t} = (-n_y, n_x)$ – unit tangent vector along the boundary Γ of Ω

u_i, v_i, w_i – Cartesian components of the displacement field in layer i

u_s, v_s, w_s – Cartesian components of the displacement field in the interlayer

\mathcal{U} – elastic strain energy

U_i, V_i, W_i – Cartesian components of the displacement field of the middle plane of layer i (intermediate-tier generalized displacements)

U_s, V_s, W_s – Cartesian components of the displacement field of the middle plane of the interlayer (intermediate-tier generalized displacements)

$U, V, W, \varphi_x, \varphi_y$ – upper-tier generalized displacements

$W_0, W_{m \cdot n}, X_0, X_{m \cdot n}, Y_0, Y_{m \cdot n}$ – constants

W_{max} – maximum deflection

W_{max}^0 – maximum deflection corresponding to zero interaction

W_{max}^∞ – maximum deflection corresponding to full interaction

z_i – coordinate that identifies the position of the middle plane of layer i

z_s – coordinate that identifies the position of the middle plane of the interlayer

Greek letters

$\alpha, \beta, \lambda, \lambda_{m \cdot n}, \rho$ – non-dimensional ratios

$\boldsymbol{\gamma}^M$ – subvector of “Mindlin” transverse shear strains (upper-tier generalized strains)

$\gamma_{xz}^M, \gamma_{yz}^M$ – “Mindlin” transverse shear strains (upper-tier generalized strains)

$\gamma_{xz,s}, \gamma_{yz,s}$ – shear strains in the interlayer

Γ – boundary of Ω

$\Gamma_{xz,s}, \Gamma_{yz,s}$ – shear strains in the interlayer (intermediate-tier generalized strains)

δ_x, δ_y – Cartesian components of the interlayer slip

Δ – relative difference

$\boldsymbol{\varepsilon}$ – column vector of upper-tier generalized strains

$\bar{\boldsymbol{\varepsilon}}$ – subvector of membrane strains (upper-tier generalized strains)

$\bar{\varepsilon}_x, \bar{\varepsilon}_y, \bar{\gamma}_{xy}$ – membrane strains (upper-tier generalized strains)

$\varepsilon_{x,i}, \varepsilon_{y,i}, \gamma_{xy,i}$ – non-zero infinitesimal strains in layer i

$\bar{\varepsilon}_{x,i}, \bar{\varepsilon}_{y,i}, \bar{\gamma}_{xy,i}$ – membrane strains in layer i (intermediate-tier generalized strains)

η, ξ – non-dimensional independent variables

$\theta_{x,s}, \theta_{y,s}$ – infinitesimal rotations of the transverse fibres of the interlayer about the y - and x -axes (left and right-handed rotations, respectively)

ν_i – Poisson ratio in the isotropy plane for the material of layer i

$\boldsymbol{\sigma}^{(a)}$ – column vector of upper-tier active generalized stresses (conjugate to the upper-tier generalized strains)

$\boldsymbol{\sigma}^{(r)}$ – column vector of upper-tier reactive generalized stress

$\sigma_{x,i}, \sigma_{y,i}, \sigma_{z,i}$ – normal stresses in layer i

$\sigma_{z,s}$ – normal stresses in the interlayer

$\tau_{xy,i}, \tau_{xz,i}, \tau_{yz,i}$ – shear stresses in layer i

$\tau_{xz,s}, \tau_{yz,s}$ – shear stresses in the interlayer

$\boldsymbol{\chi}^K, \boldsymbol{\chi}^M$ – subvector of “Kirchhoff” and “Mindlin” bending curvatures and twists (upper-tier generalized strains)

$\chi_{x,i}, \chi_{y,i}, \chi_{xy,i}$ – bending curvatures and twist in layer i (intermediate-tier generalized strains)

$\chi_x^K, \chi_y^K, \chi_{xy}^K$ – “Kirchhoff” bending curvatures and twist (upper-tier generalized strains)

$\chi_x^M, \chi_y^M, \chi_{xy}^M$ – “Mindlin” bending curvatures and twist (upper-tier generalized strains)

Ω – two-dimensional domain; bounded and simply connected open subset of \mathbb{R}^2

$\bar{\Omega}$ – closure of the set Ω in \mathbb{R}^2

Mathematical symbols

\times – Cartesian product of two sets

\cup – union of sets

\subset – is a subset of, is contained in

\in – is an element of, belongs to

∇^2 – Laplace operator in the x, y -plane

∇^4 – biharmonic operator in the x, y -plane

$\frac{\partial}{\partial x}, \frac{\partial}{\partial y}$ – partial derivatives with respect to x and with respect to y

$\frac{\partial^{n+m}}{\partial x^n \partial y^m}$ – partial derivative of order $n + m$ (with n, m non-negative integers)

\mathbb{R} – field of real numbers

$(x, y), (x, y, z)$ – ordered pair (element of \mathbb{R}^2), ordered triplet (element of \mathbb{R}^3)

$\{x\}$ – set having x as its unique element

$]x, y[$ – open interval of \mathbb{R} with extremities x and y

$[x, y]$ – closed interval of \mathbb{R} with extremities x and y

ABBREVIATIONS

CIP – Cast-in-place [resin]

EVA – Ethylene-vinyl acetate

PVB – Polyvinyl butyral

TPU – Thermoplastic polyurethane

1 INTRODUCTION

1.1 Laminated glass and its mechanical behaviour

Laminated glass consists of two or more glass plies (layers), not necessarily of equal thickness, bonded together by an adhesive interlayer to form a composite member. Such laminates have long been used in the manufacture of aircraft and automobile windshields. Their use as a structural material in the building industry has become increasingly popular over the past three decades (Schittich *et al.*, 2007) – Figures 1.1 and 1.2. Basic annealed, heat-strengthened and toughened glass can all be laminated, as can bent glass (O’Regan, 2015, p. 10). The materials used for the interlayers are polyvinyl butyral (PVB) – the one most widely used –, cast-in-place (CIP) resin, ethylene-vinyl acetate (EVA), thermoplastic polyurethane (TPU) and ionoplast (Wurm, 2007, p. 64). The number of individual glass plies that make up the laminate differ widely according to application, but in building structures the most common arrangement consists of only two plies (O’Regan, 2015, p. 10).



Figure 1.1: Apple Store – 5th Avenue, New York, 2011
(architecture: Bohlin Cywinski Jackson; structural design: Eckersley O’Callaghan)

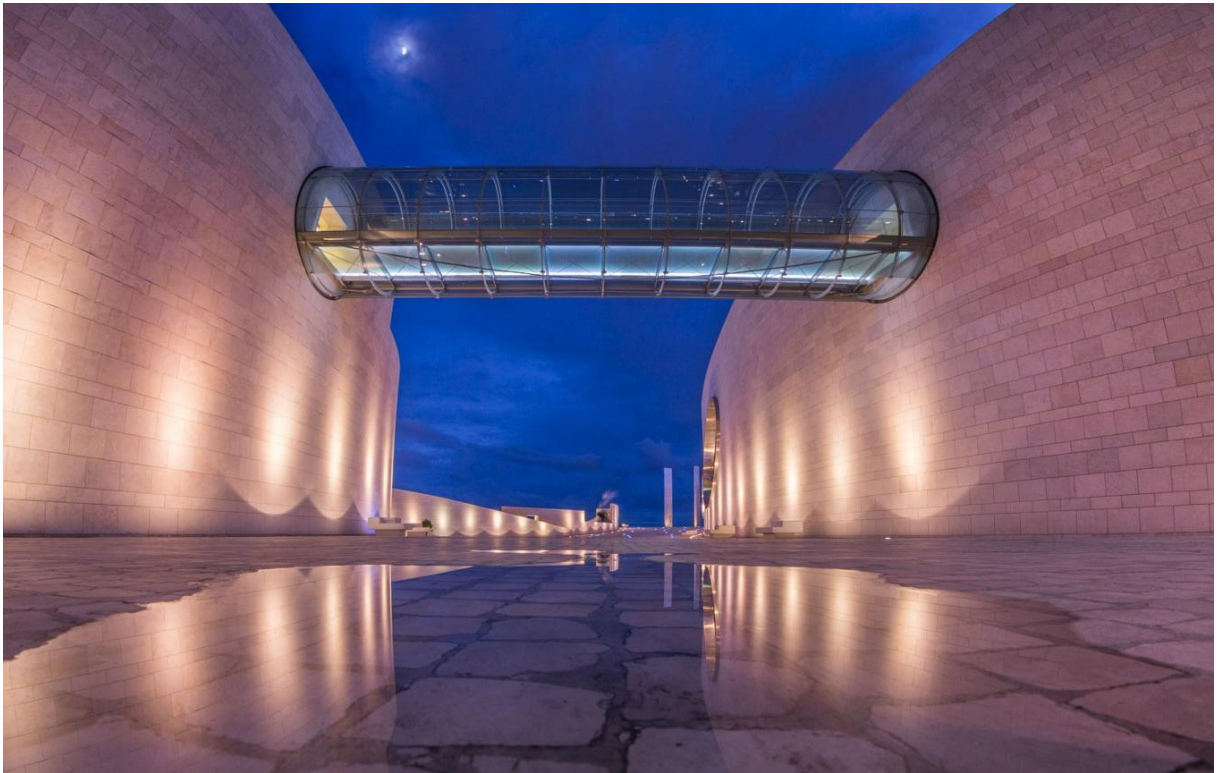


Figure 1.2: Glass bridge with a 21 m span – Champalimaud Centre for the Unknown, Lisbon, 2010
(architecture: Charles Correa Associates; structural design: Schlaich Bergermann Partner)

[photograph by Joel Santos, 2013]

The mechanical behavior of laminated glass members is greatly influenced by the presence of the interlayer (whose thickness typically ranges from 0.38 mm to 6.0 mm) and by its properties. Because of the deformability of the interlayer, there is not full interaction between consecutive glass plies, *i.e.*, the member does not behave as a monolithic, though inhomogeneous, unit. On the other hand, the assumption of zero interaction (no shear transfer between the glass plies) may be overly conservative in general. Indeed, the interlayer does restrain to some degree the relative movement of the glass plies, leading to what is commonly referred to as partial or incomplete interaction (*e.g.*, Newmark *et al.*, 1951). To complicate matters, the interlayer material is invariably a viscoelastic thermoplastic; the degree of interaction between glass plies is therefore time-dependent and highly influenced by the load history and the temperature (O'Regan, 2015, p. 10, Wurm, 2007, p. 66-67).

Laterally loaded laminated glass members can experience, prior to failure, deflections of the same order of magnitude as their own thickness, or even larger. In such cases, it is mandatory that geometrical non-linearities be accounted for.

From a structural point of view, another fundamental aspect of laminated glass is its post-breakage behaviour. When glass fractures,¹ the individual glass fragments remain adhered to the interlayer, so that a certain remaining structural capacity is obtained as the fragments lock in place, enabling compressive forces to be transmitted through the broken glass; the tensile forces are resisted by the interlayer (Haldimann *et al.*, 2008, pp. 14 and 30).

1.2 Objective and scope of the dissertation

In terms of their spatial character, many structural applications of laminated glass occur in the form of plates – flat members that exhibit one characteristic dimension, the thickness, which is much smaller than the other two. They are natural candidates to two-dimensional modelling.² In view of the preceding section, a general-purpose two-dimensional mathematical

¹ Glass is a brittle and isotropic material with an almost perfect linearly elastic behaviour up to failure. Its Young modulus E is about 70 GPa (roughly a third of that of steel) and its Poisson ratio ν can be taken between 0.22 and 0.24 (Haldimann *et al.*, 2008, p. 7). As with all brittle materials, the tensile strength of glass depends very much on surface flaws, not necessarily visible to the naked eye.

² As Andrade (2013, pp. 2-3) puts it,

“the equations describing the mechanics of a three-dimensional continuum are formidable to solve. Even in this day and age of powerful numerical techniques and high-speed, large-capacity computers, it is not feasible to treat every solid body [and every structure] as a three-dimensional continuum, at least in routine applications. This dictates the need for tractable and accurate lower-dimensional models – two-dimensional models for plates and shells, one-dimensional models for bars, either with solid cross-section or thin-walled, according to their distinctive spatial character. Massive bodies, on the other hand, are the province of the three-dimensional theories.”

Up to now, the analysis and design of laminated glass plates has relied on the use of approximate methods such as the concept of deflection- and stress-effective thicknesses – the actual laminated glass plate is replaced by “equivalent” single-layered monolithic glass ones which exhibit approximately the same maximum deflection and the same peak stresses, respectively, under equal load and support conditions (*e.g.*, Galuppi and Royer-Carfagni, 2012, Galuppi *et al.*, 2013) – or on the use of three-dimensional finite element models of varying degree of complexity (*e.g.*, Teotia and Soni, 2018).

model for the analysis of laminated glass plates – yet to be developed, to the best of the author’s knowledge – should be able to account for:

- (i) the partial interaction between glass plies;
- (ii) the viscoelastic and temperature-dependent properties of the interlayer;
- (iii) geometrical non-linearities;
- (iv) quasi-static and dynamic loads, as well as indirect actions (such as temperature changes and support settlements);
- (v) realistic failure criteria.

Moreover, the model should be able to represent accurately the supports and fixings used in actual construction practice, as the brittle nature of glass makes it extremely susceptible to stress concentrations (*e.g.*, Dias da Silva, 2006, §VI.9).

Such a list of requirements constitutes, in fact, the outline of a research program, but one that is obviously not feasible to carry out within the time constraints of a single MSc dissertation. As a first step along that road, the aim of the present work is to model two-dimensionally the partial interaction behaviour of two-layer plates acted by quasi-static loads and prescribed support displacements, in a geometrically and materially linear context and at constant temperature. The point of departure is the key assumption that each layer (*resp.* the interlayer), when considered separately, behaves as a Kirchhoff plate (*resp.* as a transverse shear-only Mindlin plate).

It may seem at first glance that such a first step overlaps entirely with the work of Foraboschi (2012), but that is not so, as there are important conceptual differences:

- (i) Some of Foraboschi’s assumptions are mutually contradictory and cannot be reconciled with the three-dimensional theory of linear elasticity:
 - The assumptions of isotropic linearly elastic material behaviour and inextensibility of transverse fibres are inconsistent with the assumption of zero transverse normal stresses (in each layer and in the interlayer).
 - Equilibrium inconsistencies arise from the assumptions of isotropic linearly elastic material behaviour and zero shear strains (in each layer).

In the present dissertation, inconsistencies of this sort – which, it must be said, are not uncommon in the literature on structural mechanics – are avoided by the adoption of the method of internal constraints (essentially due to Podio-Guidugli, 1989) to achieve the reduction in the number of spatial dimensions from three to just two. A complete characterization of the stress state, split into active and reactive parts, is also obtained. In fact, this dissertation can be seen as an extension of the work of Lembo and Podio-Guidugli (1991), who used the method of internal constraints to derive consistently, from three-dimensional linear elasticity, the two-dimensional equations of multi-layered Kirchhoff plates with full interaction.

- (ii) Foraboschi's definition of the transverse shear strains in the interlayer as the quotient of the relative displacements, parallel to the middle plane, between the end faces of the interlayer (which he identifies with the slip) by the thickness of the interlayer is shown to be incorrect and modified appropriately.

Additional distinctive and novel features of the model presented in this dissertation, which increase its range of applicability, include the consideration of layers with unequal thicknesses and/or made of different materials (as in the case of glass and polycarbonate layers joined by a TPU interlayer) and making allowance for applied forces parallel to the middle plane of the plate. Finally, a judicious choice of generalized displacements, motivated by Gjelsvik's (1991) work on composite beams, brings to centre stage a number of illuminating similarities with the plate theories of Kirchhoff and Mindlin (in fact, it might be suggestively said that the model presented in this dissertation is an amalgamation of these two classical theories).

1.3 Outline of the dissertation

This document is organized into four chapters.

The first chapter – the present introduction – sets out the objective and the scope of the dissertation, which are motivated and placed in context by a brief literature review.

Chapter 2 constitutes the bulk of the dissertation. It presents a consistent derivation, from three-dimensional linear elasticity, of a two-dimensional mathematical model describing the bending and in-plane stretching behaviours, under a general system of quasi-static

distributed loads, of thin two-layer plates with partial shear interaction. Two appendices supplement this chapter. Appendix 1 summarizes, in the form of a Tonti diagram, the two-dimensional field equations of the model. Appendix 2 gives an explicit characterization of the reactive stresses (*i.e.*, of those stresses that are not determined by the strains, but ensure that equilibrium is satisfied everywhere).

In chapter 3, a problem with closed-form analytical solution illustrates the application of the two-dimensional model and its capabilities. Moreover, such an analytical solution will surely prove useful in the future as a benchmark for verifying computational models.³ The problem is then generalized and a Navier-type solution (*i.e.*, a solution in the form of truncated double trigonometric series) is obtained. The results are compared with those reported by Foraboschi (2012) and it is found that significant differences may occur.

Finally, chapter 4 provides a summary of the conclusions drawn from this work, emphasizing the main findings. Some suggestions for future research, which revisit the program set out at the beginning of section 1.2, are also made.

³ Verification is here understood as “the process of determining if a computational model obtained by discretizing a mathematical model of a physical event and the code implementing the computational model can be used to represent the mathematical model of the event with sufficient accuracy” (Babuska and Oden, 2004).

2 TWO-DIMENSIONAL MATHEMATICAL MODEL

2.1 Preliminary considerations

A fixed right-handed Cartesian coordinate system, with axes x , y and z , is chosen in three-dimensional Euclidean space, which will therefore be identified with \mathbb{R}^3 .

We consider a plate formed by two superposed parallel layers, labelled 1 and 2, each of which is, in itself, a plate-like body with uniform thickness. These two layers are connected by a thin interlayer, also with uniform thickness (Figure 2.1). In the absence of applied loads, each layer i ($i = 1, 2$) occupies the reference configuration $\bar{\Omega} \times [z_i - \frac{1}{2}h_i, z_i + \frac{1}{2}h_i]$, where

- (i) $\Omega \subset \mathbb{R}^2$ is a bounded and simply connected open set with boundary Γ , which we take to be a piecewise regular Jordan curve, and $\bar{\Omega} = \Omega \cup \Gamma$ is the closure of Ω in \mathbb{R}^2 ;⁴
- (ii) h_i is the (small) thickness of the layer;
- (iii) the coordinate $z = z_i$ identifies the position of the layer's middle plane.

For definiteness, we take $z_2 > z_1$. We may think of the z -axis as being “vertical” and pointing “downwards”, in which case we refer to layer 1 as the “top” layer and to layer 2 as the “bottom” layer. The reference configuration of the interlayer is the set $\bar{\Omega} \times [z_s - \frac{1}{2}h_s, z_s + \frac{1}{2}h_s]$, where $h_s = z_2 - z_1 - \frac{1}{2}(h_1 + h_2) > 0$ and $z_s = \frac{1}{2}(z_1 + z_2) + \frac{1}{4}(h_1 - h_2)$.

The construction of the mathematical model is organized in terms of a three-tier hierarchy:

- (i) At the bottom, each of the layers and the interlayer are regarded as separate three-dimensional continuum bodies, governed by the linear theory of elasticity.

⁴ Since Γ is a piecewise regular Jordan curve, we can define the unit outer normal vector $\mathbf{n} = (n_x, n_y)$ and the unit tangent vector $\mathbf{t} = (-n_y, n_x)$, oriented in the usual way, almost everywhere along Γ (Figure 2.1).

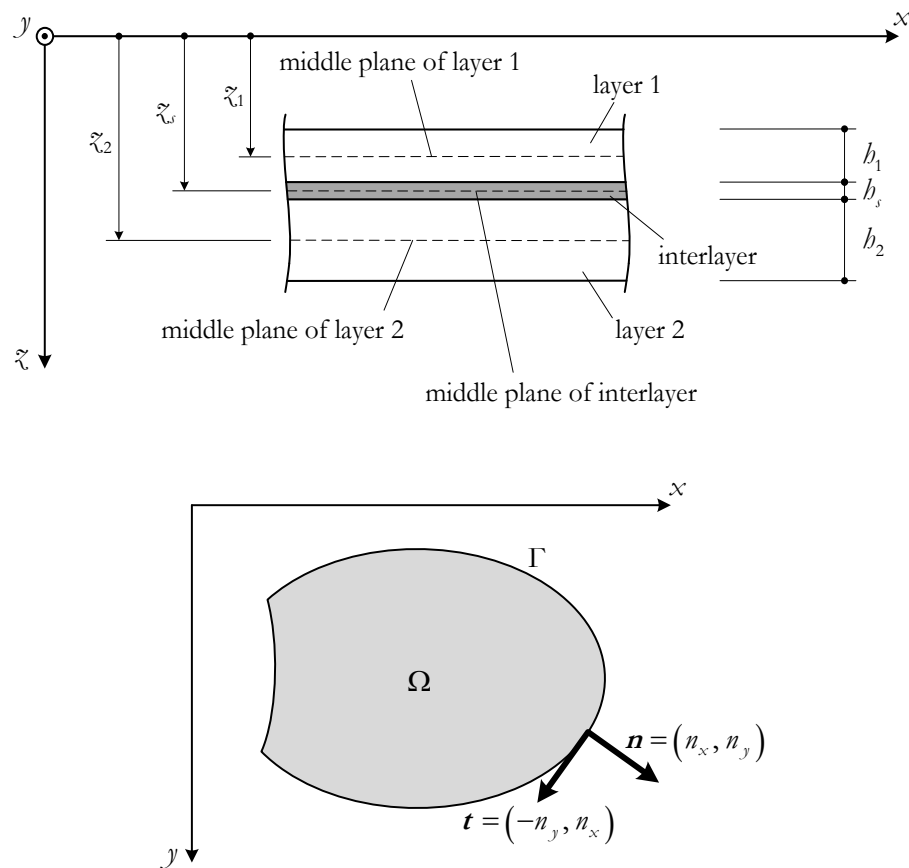


Figure 2.1: Two-layer plate – Cartesian coordinate system and reference configuration

- (ii) At an intermediate level, the two layers and the interlayer are still considered separately, but now they are described by two-dimensional equations.
- (iii) At the top seats the layered plate, regarded as a single two-dimensional composite member.

Accordingly, there are two steps involved in the process. The first step is one of dimensional reduction and the tool we use to take it, in a consistent manner, is the method of internal constraints, essentially due to Podio-Guidugli (1989). The second step is one of assembly or aggregation, somewhat reminiscent of the finite element method, in which the continuity of displacements and certain stress components across each layer/interlayer interface is enforced.

2.2 Assumptions

The fundamental assumptions employed in the construction of the mathematical model are the following:

- (A1) Displacements are small (their derivatives are negligible in comparison with unity).
- (A2) Each layer is bonded to the interlayer in such a way that both sliding and detachment are prevented, thus the displacement field is continuous on $\bar{\Omega} \times [z_1 - \frac{1}{2}h_1, z_2 + \frac{1}{2}h_2]$.
- (A3) Each layer, individually considered, behaves as a linearly elastic Kirchhoff plate: fibres initially normal to its middle plane $\bar{\Omega} \times \{z_i\}$ remain, after deformation, (A3.1) straight and normal to the deformed middle plane and (A3.2) unstretched (to within the first order). In other words, the said fibres undergo infinitesimal rigid displacements (Gurtin, 1981, pp. 55-56), remaining normal to the deformed middle plane.
- (A4) The interlayer, individually considered, behaves as a linearly elastic Mindlin plate: fibres initially normal to its middle plane $\bar{\Omega} \times \{z_s\}$ remain, after deformation, (A4.1) straight and (A4.2) unstretched (to within the first order). In other words, the said fibres undergo infinitesimal rigid displacements, but do not necessarily remain normal to the deformed middle plane.

Adopting the point of view of Lembo and Podio-Guidugli (1991) and Nardinocchi & Podio-Guidugli (1994), we give the Kirchhoff assumptions A3.1-A3.2 and the Mindlin assumption A4.2 the status of internal constraints, that is, “*constitutive* prescriptions restricting the class of possible deformations” [italics added] (see also Podio-Guidugli, 1989, and Lembo, 1989). Transverse isotropy is the maximal material symmetry compatible with the constraint of inextensibility of transverse fibres, either taken in isolation (as in the interlayer) or in conjunction with the constraint of preservation of orthogonality between those same fibres and the middle plane (as in each of the two layers). This often overlooked fact leads to the adoption of the following additional assumption:

- (A5) The constituent materials are homogeneous⁵ and transversely isotropic, with the z -direction being the direction of monotropy.

⁵ The homogeneity assumption is not essential and could easily be relaxed.

Two further assumptions complete this enumeration:

(A6) The interlayer material is modelled as a transverse shear-only material (*e.g.*, Hooper, 1973) – its stress response to deformation is such that no significant in-plane stresses $\sigma_{x,s}$, $\sigma_{y,s}$ and $\tau_{xy,s}$ are generated and so the Young and shear moduli in the x, y -plane of isotropy are taken to be zero.

(A7) The reference configuration corresponds to a natural state (*i.e.*, there are no residual stresses).

2.3 Kinematics

In a geometrically linear framework (assumption A1), the Cartesian components of the displacement field in layer i ($i = 1, 2$) must satisfy the conditions

$$\frac{\partial}{\partial z} w_i(x, y, z) = 0 \quad (1)$$

$$\frac{\partial}{\partial z} u_i(x, y, z) + \frac{\partial}{\partial x} w_i(x, y, z) = 0 \quad (2)$$

$$\frac{\partial}{\partial z} v_i(x, y, z) + \frac{\partial}{\partial y} w_i(x, y, z) = 0, \quad (3)$$

which express in mathematical terms the Kirchhoff constraints A3.2 and A3.1. The general solution of this system of partial differential equations is of the form

$$u_i(x, y, z) = U_i(x, y) - (z - z_i) \frac{\partial W_i}{\partial x}(x, y) \quad (4)$$

$$v_i(x, y, z) = V_i(x, y) - (z - z_i) \frac{\partial W_i}{\partial y}(x, y) \quad (5)$$

$$w_i(x, y, z) = W_i(x, y), \quad (x, y) \in \bar{\Omega}, \quad z \in \left[z_i - \frac{1}{2} h_i, z_i + \frac{1}{2} h_i \right], \quad i = 1, 2, \quad (6)$$

where U_i, V_i and W_i , which are functions of x and y alone, represent the Cartesian components of the displacement field of the middle plane of layer i (Figure 2.2).

As for the Cartesian components of the displacement field in the interlayer, they must satisfy the conditions

$$\frac{\partial}{\partial z} w_s(x, y, z) = 0 \quad (7)$$

$$\frac{\partial}{\partial z} \left(\frac{\partial}{\partial z} u_s(x, y, z) + \frac{\partial}{\partial x} w_s(x, y, z) \right) = 0 \quad (8)$$

$$\frac{\partial}{\partial z} \left(\frac{\partial}{\partial z} v_s(x, y, z) + \frac{\partial}{\partial y} w_s(x, y, z) \right) = 0, \quad (9)$$

which put in force the Mindlin assumptions A4.2 and A4.1. The general solution of the system (7)-(9) is

$$u_s(x, y, z) = U_s(x, y) - (z - z_s)\theta_{x,s}(x, y) \quad (10)$$

$$v_s(x, y, z) = V_s(x, y) - (z - z_s)\theta_{y,s}(x, y) \quad (11)$$

$$w_s(x, y, z) = W_s(x, y), (x, y) \in \bar{\Omega}, z \in \left[z_s - \frac{1}{2}h_s, z_s + \frac{1}{2}h_s \right], \quad (12)$$

where U_s, V_s, W_s once again represent the Cartesian components of the displacement field of the middle plane of the interlayer and $\theta_{x,s}, \theta_{y,s}$ represent the (infinitesimal) rotations of the transverse fibres about the y - and x -axes (left and right-handed rotations, respectively).

In conclusion, at the intermediate tier of the hierarchy set forth above, we have a total of eleven generalized displacements (*i.e.*, scalar fields with domain $\bar{\Omega} \subset \mathbb{R}^2$ that parametrise the three-dimensional displacement fields (4)-(6) and (10)-(12)).

To join together layers and interlayer into a single composite member and thereby reach the upper tier, we use assumption A2 and impose the continuity conditions

$$u_i \left(x, y, z_i + (-1)^{i+1} \frac{1}{2}h_i \right) = u_s \left(x, y, z_s + (-1)^i \frac{1}{2}h_s \right) \quad (13)$$

$$v_i \left(x, y, z_i + (-1)^{i+1} \frac{1}{2}h_i \right) = v_s \left(x, y, z_s + (-1)^i \frac{1}{2}h_s \right) \quad (14)$$

$$w_i \left(x, y, z_i + (-1)^{i+1} \frac{1}{2}h_i \right) = w_s \left(x, y, z_s + (-1)^i \frac{1}{2}h_s \right), (x, y) \in \bar{\Omega}, i = 1, 2. \quad (15)$$

From (15) we conclude at once that

$$W_1 = W_2 = W_s \quad (16)$$

and this common transverse displacement will be denoted simply by W . Drawing inspiration from Gjelsvik (1991) (see also Ferreira *et al.*, 2018, and Andrade *et al.*, 2019), we further define

$$U = \frac{1}{z_2 - z_1} (z_2 U_1 - z_1 U_2) \quad V = \frac{1}{z_2 - z_1} (z_2 V_1 - z_1 V_2) \quad (17)$$

$$\varphi_x = \frac{1}{z_2 - z_1} (U_1 - U_2) \quad \varphi_y = \frac{1}{z_2 - z_1} (V_1 - V_2), \quad (18)$$

so that

$$U_i = U - z_i \varphi_x \quad V_i = V - z_i \varphi_y, \quad i = 1, 2. \quad (19)$$

It then follows from (13)-(14) that

$$U_s = U + \frac{h_2 - h_1}{4} \frac{\partial W}{\partial x} - \frac{z_1 + z_2}{2} \varphi_x \quad V_s = V + \frac{h_2 - h_1}{4} \frac{\partial W}{\partial y} - \frac{z_1 + z_2}{2} \varphi_y \quad (20)$$

$$\theta_{x,s} = -\frac{h_1 + h_2}{2h_s} \frac{\partial W}{\partial x} + \frac{z_2 - z_1}{h_s} \varphi_x \quad \theta_{y,s} = -\frac{h_1 + h_2}{2h_s} \frac{\partial W}{\partial y} + \frac{z_2 - z_1}{h_s} \varphi_y. \quad (21)$$

Therefore, we have a total of five upper-tier generalized displacements – namely U , V , W , φ_x and φ_y –, whose geometrical meaning is illustrated in Figure 2.2 and in terms of which (4)-(6) and (10)-(12) can be rewritten as

$$u_i = U - (z - z_i) \frac{\partial W}{\partial x} - z_i \varphi_x \quad (22)$$

$$v_i = V - (z - z_i) \frac{\partial W}{\partial y} - z_i \varphi_y \quad (23)$$

$$w_i = W, \quad i = 1, 2 \quad (24)$$

$$u_s = U + \left[\frac{h_2 - h_1}{4} + (z - z_s) \frac{h_1 + h_2}{2h_s} \right] \frac{\partial W}{\partial x} - \left[\frac{z_1 + z_2}{2} + (z - z_s) \frac{z_2 - z_1}{h_s} \right] \varphi_x \quad (25)$$

$$v_s = V + \left[\frac{h_2 - h_1}{4} + (z - z_s) \frac{h_1 + h_2}{2h_s} \right] \frac{\partial W}{\partial y} - \left[\frac{z_1 + z_2}{2} + (z - z_s) \frac{z_2 - z_1}{h_s} \right] \varphi_y \quad (26)$$

$$w_s = W. \quad (27)$$

In (24) and (27) we are committing a harmless and rather convenient notational abuse, by identifying functions with different domains.

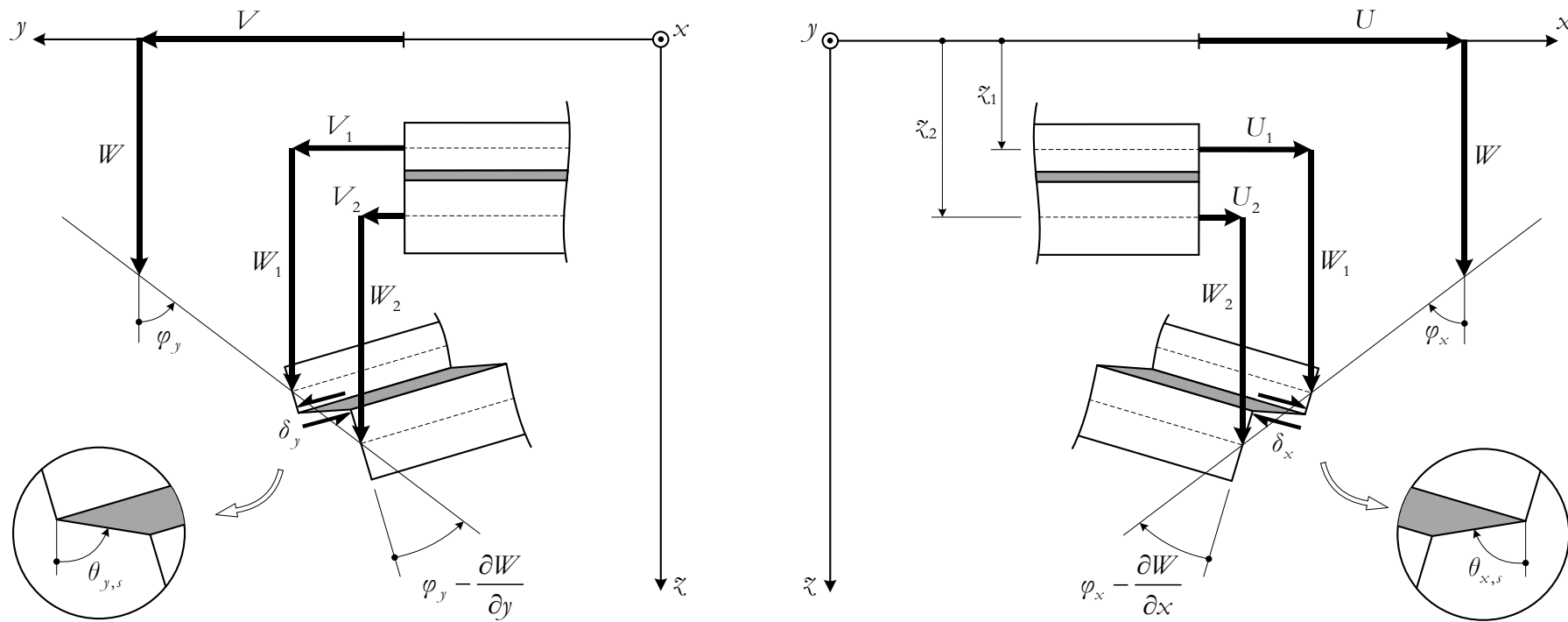


Figure 2.2: Displacement field

The non-vanishing Cartesian components of the (infinitesimal) strain tensor field corresponding to the displacement field (4)-(6) in each layer are

$$\varepsilon_{x,i} = \frac{\partial u_i}{\partial x} = \frac{\partial U_i}{\partial x} - (z - z_i) \frac{\partial^2 W_i}{\partial x^2} \quad (28)$$

$$\varepsilon_{y,i} = \frac{\partial v_i}{\partial y} = \frac{\partial V_i}{\partial y} - (z - z_i) \frac{\partial^2 W_i}{\partial y^2} \quad (29)$$

$$2\varepsilon_{xy,i} = \gamma_{xy,i} = \frac{\partial u_i}{\partial y} + \frac{\partial v_i}{\partial x} = \frac{\partial U_i}{\partial y} + \frac{\partial V_i}{\partial x} - 2(z - z_i) \frac{\partial^2 W_i}{\partial x \partial y}, \quad i = 1, 2. \quad (30)$$

Consequently, the membrane strains

$$\bar{\varepsilon}_{x,i} = \frac{\partial U_i}{\partial x} \quad \bar{\varepsilon}_{y,i} = \frac{\partial V_i}{\partial y} \quad \bar{\gamma}_{xy,i} = \frac{\partial U_i}{\partial y} + \frac{\partial V_i}{\partial x}, \quad (31)$$

the bending curvatures

$$\chi_{x,i} = -\frac{\partial^2 W_i}{\partial x^2} \quad \chi_{y,i} = -\frac{\partial^2 W_i}{\partial y^2} \quad (32)$$

and the twist

$$\chi_{xy,i} = -2 \frac{\partial^2 W_i}{\partial x \partial y} \quad (33)$$

provide a complete two-dimensional description of the state of strain in each layer i . They are adopted as intermediate-tier generalized strains.

Let us now examine the state of strain in the interlayer. From (10)-(12) we find the non-zero strain fields

$$\varepsilon_{x,s} = \frac{\partial u_s}{\partial x} = \frac{\partial U_s}{\partial x} - (z - z_s) \frac{\partial \theta_{x,s}}{\partial x} \quad (34)$$

$$\varepsilon_{y,s} = \frac{\partial v_s}{\partial y} = \frac{\partial V_s}{\partial y} - (z - z_s) \frac{\partial \theta_{y,s}}{\partial y} \quad (35)$$

$$2\varepsilon_{xy,s} = \gamma_{xy,s} = \frac{\partial u_s}{\partial y} + \frac{\partial v_s}{\partial x} = \frac{\partial U_s}{\partial y} + \frac{\partial V_s}{\partial x} - (z - z_s) \left(\frac{\partial \theta_{x,s}}{\partial y} + \frac{\partial \theta_{y,s}}{\partial x} \right) \quad (36)$$

$$2\varepsilon_{xz,s} = \gamma_{xz,s} = \frac{\partial u_s}{\partial z} + \frac{\partial w_s}{\partial x} = \frac{\partial W_s}{\partial x} - \theta_{x,s} \quad (37)$$

$$2\varepsilon_{yz,s} = \gamma_{yz,s} = \frac{\partial v_s}{\partial z} + \frac{\partial w_s}{\partial y} = \frac{\partial W_s}{\partial y} - \theta_{y,s}. \quad (38)$$

Of these, and by virtue of assumption A6, only the transverse shear strains $\gamma_{xz,s}$ and $\gamma_{yz,s}$ will play a role in the derivation of the two-dimensional model. Moreover, $\gamma_{xz,s}$ and $\gamma_{yz,s}$ are constant across the thickness of the interlayer, as implied by A4.1. We conclude that the description of strain in the interlayer at the intermediate tier requires only two generalized strains, the transverse shearing angles (37)-(38). To accentuate the distinction between bottom and intermediate tiers, we use the notation

$$\Gamma_{xz,s} = \frac{\partial W_s}{\partial x} - \theta_{x,s} \quad \Gamma_{yz,s} = \frac{\partial W_s}{\partial y} - \theta_{y,s} \quad (39)$$

when positioning ourselves at the latter.

We now plug (16), (19) and (21) into (28)-(30) and (37)-(38) to obtain

$$\varepsilon_{x,i} = \frac{\partial U}{\partial x} - (z - z_i) \frac{\partial^2 W}{\partial x^2} - z_i \frac{\partial \varphi_x}{\partial x} \quad (40)$$

$$\varepsilon_{y,i} = \frac{\partial V}{\partial y} - (z - z_i) \frac{\partial^2 W}{\partial y^2} - z_i \frac{\partial \varphi_y}{\partial y} \quad (41)$$

$$\gamma_{xy,i} = \frac{\partial U}{\partial y} + \frac{\partial V}{\partial x} - 2(z - z_i) \frac{\partial^2 W}{\partial x \partial y} - z_i \left(\frac{\partial \varphi_x}{\partial y} + \frac{\partial \varphi_y}{\partial x} \right), \quad i = 1, 2 \quad (42)$$

$$\gamma_{xz,s} = \frac{z_2 - z_1}{h_s} \left(\frac{\partial W}{\partial x} - \varphi_x \right) \quad (43)$$

$$\gamma_{yz,s} = \frac{z_2 - z_1}{h_s} \left(\frac{\partial W}{\partial y} - \varphi_y \right). \quad (44)$$

This prompts the adoption of

$$\bar{\varepsilon}_x = \frac{\partial U}{\partial x} \quad \bar{\varepsilon}_y = \frac{\partial V}{\partial y} \quad \bar{\gamma}_{xy} = \frac{\partial U}{\partial y} + \frac{\partial V}{\partial x} \quad (45)$$

$$\chi_x^K = -\frac{\partial^2 W}{\partial x^2} \quad \chi_y^K = -\frac{\partial^2 W}{\partial y^2} \quad \chi_{xy}^K = -2 \frac{\partial^2 W}{\partial x \partial y} \quad (46)$$

$$\chi_x^M = -\frac{\partial \varphi_x}{\partial x} \quad \chi_y^M = -\frac{\partial \varphi_y}{\partial y} \quad \chi_{xy}^M = -\left(\frac{\partial \varphi_x}{\partial y} + \frac{\partial \varphi_y}{\partial x} \right) \quad (47)$$

$$\gamma_{xz}^M = \frac{\partial W}{\partial x} - \varphi_x \quad \gamma_{yz}^M = \frac{\partial W}{\partial y} - \varphi_y \quad (48)$$

as the eleven generalized strains at the top tier of the hierarchy. The superscripts “ K ” and “ M ” are intended to emphasize the similarities with the Kirchhoff (1850, 1876) and Mindlin (1951) plate bending theories. For completeness, we note the following relations:

$$\bar{\varepsilon}_{x,i} = \bar{\varepsilon}_x + z_i \chi_x^M \quad \bar{\varepsilon}_{y,i} = \bar{\varepsilon}_y + z_i \chi_y^M \quad \bar{\gamma}_{xy,i} = \bar{\gamma}_{xy} + z_i \chi_{xy}^M \quad (49)$$

$$\chi_{x,i} = \chi_x^K \quad \chi_{y,i} = \chi_y^K \quad \chi_{xy,i} = \chi_{xy}^K, \quad i = 1, 2 \quad (50)$$

$$\Gamma_{xz,s} = \frac{z_2 - z_1}{h_s} \gamma_{xz}^M \quad \Gamma_{yz,s} = \frac{z_2 - z_1}{h_s} \gamma_{yz}^M. \quad (51)$$

The interaction between the layers that form a composite member is often characterized in the literature in terms of their relative slip (*e.g.*, Newmark *et al.*, 1951): zero slip corresponds to full interaction (*i.e.*, monolithic behaviour, meaning that fibres initially normal to the x , y -plane remain straight across the entire thickness of the layered plate), free slip corresponds to no interaction and, between these two limits, the situation is one of partial interaction (slip is restrained to a varying degree but not entirely prevented). In our model, the components δ_x and δ_y of the relative slip between the two layers (Figure 2.2), are defined by

$$\delta_x = -h_s \Gamma_{xz,s} = -(z_2 - z_1) \left(\frac{\partial W}{\partial x} - \varphi_x \right) \quad (52)$$

$$\delta_y = -h_s \Gamma_{yz,s} = -(z_2 - z_1) \left(\frac{\partial W}{\partial y} - \varphi_y \right). \quad (53)$$

Observe that

$$\delta_x(x, y) = u_1 \left(x, y, z_1 + \frac{1}{2} h_1 \right) - u_2 \left(x, y, z_2 - \frac{1}{2} h_2 \right) - h_s \frac{\partial W}{\partial x}(x, y) \quad (54)$$

$$\delta_y(x, y) = v_1 \left(x, y, z_1 + \frac{1}{2} h_1 \right) - v_2 \left(x, y, z_2 - \frac{1}{2} h_2 \right) - h_s \frac{\partial W}{\partial y}(x, y). \quad (55)$$

Unless the interlayer thickness is negligible, the slip components cannot be defined merely on the basis of the relative displacements, in the x - and y -directions, between the “bottom” face of layer 1 and the “top” face of layer 2. The additional term $-h_s \frac{\partial W}{\partial x}$ (resp. $-h_s \frac{\partial W}{\partial y}$) is necessary to ensure that $\delta_x = 0$ (resp. $\delta_y = 0$) if and only if $\varphi_x = \frac{\partial W}{\partial x}$ (resp. $\varphi_y = \frac{\partial W}{\partial y}$). Unlike Galuppi and Royer-Carfagni (2012), Foraboschi (2012) overlooks this point and the oversight carries over into the definition of the transverse shear stresses in the interlayer.

2.4 Constitutive equations

According to the principle of determinism for internally constrained materials, the symmetric stress tensor fields on each layer and on the interlayer are split additively into reactive and active parts, also symmetric. The former, whose role is to maintain the constraints and ensure that equilibrium is satisfied, do no work in any admissible deformation. We have seen that the Kirchhoff constraints in force on each layer i restrict their possible deformations to those characterized by $\varepsilon_{z,i} = \gamma_{xz,i} = \gamma_{yz,i} = 0$. The corresponding stress components – the normal stress $\sigma_{z,i}$ and the shear stresses $\tau_{xz,i}$ and $\tau_{yz,i}$ – are reactive. Similarly, the transverse inextensibility constraint in force on the interlayer restricts its possible deformations to those with $\varepsilon_{z,s} = 0$. The corresponding stress component – the normal stress $\sigma_{z,s}$ – is reactive. The remaining stress components are active and hence determined by an appropriate stress-strain law.

Each layer is made of a homogeneous, linearly elastic and transversely isotropic material, with z as the direction of monotropy (assumption A5), internally constrained according to A3.1 and A3.2 and without residual stresses (assumption A7). Let the material of layer i have Young modulus E_i and Poisson ratio ν_i in the isotropy plane. Then the active stresses are related to the strains via (Lembo and Podio-Guidugli, 1991)

$$\sigma_{x,i} = \frac{E_i}{1-\nu_i^2} (\varepsilon_{x,i} + \nu_i \varepsilon_{y,i}) \quad (56)$$

$$\sigma_{y,i} = \frac{E_i}{1-\nu_i^2} (\varepsilon_{y,i} + \nu_i \varepsilon_{x,i}) \quad (57)$$

$$\tau_{xy,i} = \frac{E_i}{2(1+\nu_i)} \gamma_{xy,i}, \quad i = 1, 2. \quad (58)$$

⁶ In compliance form, Hooke's law for an *unconstrained* transversely isotropic material (with z as the direction of monotropy) reads (e.g., Dias da Silva, 2006, § IV.4.c)

$$\begin{aligned} \varepsilon_{x,i} &= \frac{1}{E_i} \sigma_{x,i} - \frac{\nu_i}{E_i} \sigma_{y,i} - \frac{\nu_{zx,i}}{E_{z,i}} \sigma_{z,i} \\ \varepsilon_{y,i} &= -\frac{\nu_i}{E_i} \sigma_{x,i} + \frac{1}{E_i} \sigma_{y,i} - \frac{\nu_{zy,i}}{E_{z,i}} \sigma_{z,i} \\ \varepsilon_{z,i} &= -\frac{\nu_{xz,i}}{E_i} \sigma_{x,i} - \frac{\nu_{yz,i}}{E_i} \sigma_{y,i} + \frac{1}{E_{z,i}} \sigma_{z,i} \\ \gamma_{xy,i} &= \frac{2(1+\nu_i)}{E_i} \tau_{xy,i} \\ \gamma_{xz,i} &= \frac{1}{G_{z,i}} \tau_{xz,i} \\ \gamma_{yz,i} &= \frac{1}{G_{z,i}} \tau_{yz,i}, \end{aligned}$$

The interlayer material is also assumed to be homogeneous, linearly elastic and transversely isotropic, with z as the direction of anisotropy. Moreover, the Young and shear moduli in the x, y -plane of isotropy are taken to be zero – assumption A6. This leaves the transverse shear stresses, $\tau_{xz,s}$ and $\tau_{yz,s}$, as the only non-zero active stress components. They are given by the constitutive law

$$\tau_{xz,s} = G_{z,s} \gamma_{xz,s} \quad \tau_{yz,s} = G_{z,s} \gamma_{yz,s}, \quad (59)$$

where $G_{z,s}$ is the relevant shear modulus (with $0 \leq G_{z,s} < +\infty$)⁷. They are independent of z , *i.e.*, they do not vary across the interlayer thickness.

At the intermediate level of the three-tier hierarchy, the active generalized stresses are the through-the-thickness resultants of the active stresses in each layer and in the interlayer. Written as functions of either the 14 intermediate-tier generalized strains (31)-(33) and (39) or the 11 top-tier generalized strains (45)-(48), we have the membrane forces

$$N_{x,i} = \int_{z_i - \frac{1}{2}h_i}^{z_i + \frac{1}{2}h_i} \sigma_{x,i} dz = \frac{E_i h_i}{1-\nu_i^2} (\bar{\varepsilon}_{x,i} + \nu_i \bar{\varepsilon}_{y,i}) = \frac{E_i h_i}{1-\nu_i^2} \left[\bar{\varepsilon}_x + z_i \chi_x^M + \nu_i (\bar{\varepsilon}_y + z_i \chi_y^M) \right] \quad (60)$$

$$N_{y,i} = \int_{z_i - \frac{1}{2}h_i}^{z_i + \frac{1}{2}h_i} \sigma_{y,i} dz = \frac{E_i h_i}{1-\nu_i^2} (\bar{\varepsilon}_{y,i} + \nu_i \bar{\varepsilon}_{x,i}) = \frac{E_i h_i}{1-\nu_i^2} \left[\bar{\varepsilon}_y + z_i \chi_y^M + \nu_i (\bar{\varepsilon}_x + z_i \chi_x^M) \right] \quad (61)$$

$$N_{xy,i} = \int_{z_i - \frac{1}{2}h_i}^{z_i + \frac{1}{2}h_i} \tau_{xy,i} dz = \frac{E_i h_i}{2(1+\nu_i)} \bar{\gamma}_{xy,i} = \frac{E_i h_i}{2(1+\nu_i)} (\bar{\gamma}_{xy} + z_i \chi_{xy}^M), \quad (62)$$

with

$$\nu_{zx,i} = \nu_{zy,i} \quad \nu_{xz,i} = \nu_{yz,i} \quad \frac{\nu_{xz,i}}{E_i} = \frac{\nu_{zx,i}}{E_{z,i}}$$

There are therefore five independent material parameters.

To ensure that $\varepsilon_{z,i} = 0$ regardless of $\sigma_{x,i}$, $\sigma_{y,i}$ and $\sigma_{z,i}$, as required by the internal constraint A3.2, the compliance $\frac{1}{E_{z,i}}$ must vanish. Similarly, we must set $\frac{1}{G_{z,i}} = 0$ so as to have $\gamma_{xz,i} = \gamma_{yz,i} = 0$ regardless of $\tau_{xz,i}$ and $\tau_{yz,i}$, as required by the internal constraint A3.1. Then, writing the first, second and fourth equations in stiffness form, we obtain (56)-(58) for the internally constrained material, with just two independent material parameters.

⁷ The case $G_{z,s} = 0$ corresponds to zero interaction between the layers; the limit as $G_{z,s} \rightarrow +\infty$ corresponds to full interaction (monolithic behaviour).

the bending moments

$$M_{x,i} = \int_{z_i - \frac{1}{2}h_i}^{z_i + \frac{1}{2}h_i} (z - z_i) \sigma_{x,i} dz = \frac{E_i h_i^3}{12(1-\nu_i^2)} (\chi_{x,i} + \nu_i \chi_{y,i}) = \frac{E_i h_i^3}{12(1-\nu_i^2)} (\chi_x^K + \nu_i \chi_y^K) \quad (63)$$

$$M_{y,i} = \int_{z_i - \frac{1}{2}h_i}^{z_i + \frac{1}{2}h_i} (z - z_i) \sigma_{y,i} dz = \frac{E_i h_i^3}{12(1-\nu_i^2)} (\chi_{y,i} + \nu_i \chi_{x,i}) = \frac{E_i h_i^3}{12(1-\nu_i^2)} (\chi_y^K + \nu_i \chi_x^K) \quad (64)$$

and the twisting moment

$$M_{xy,i} = \int_{z_i - \frac{1}{2}h_i}^{z_i + \frac{1}{2}h_i} (z - z_i) \tau_{xy,i} dz = \frac{E_i h_i^3}{24(1+\nu_i)} \chi_{xy,i} = \frac{E_i h_i^3}{24(1+\nu_i)} \chi_{xy}^K \quad (65)$$

in each of the two layers ($i = 1, 2$), and the transverse shear forces

$$Q_{x,s} = \int_{z_s - \frac{1}{2}h_s}^{z_s + \frac{1}{2}h_s} \tau_{xz,s} dz = G_s h_s \Gamma_{xz,s} = G_{z,s} (z_2 - z_1) \gamma_{xz}^M \quad (66)$$

$$Q_{y,s} = \int_{z_s - \frac{1}{2}h_s}^{z_s + \frac{1}{2}h_s} \tau_{yz,s} dz = G_s h_s \Gamma_{yz,s} = G_{z,s} (z_2 - z_1) \gamma_{yz}^M \quad (67)$$

in the interlayer.

Finally, at the top tier of the hierarchy, we define eleven active generalized stresses for the whole of the layered plate by requiring that they be energy-conjugate to the eleven top-tier generalized strains (45)-(48). Specifically, we write the elastic strain energy stored in the member,

$$\begin{aligned} \mathcal{U} = & \frac{1}{2} \iint_{\Omega} \left[\sum_{i=1}^2 \int_{z_i - \frac{1}{2}h_i}^{z_i + \frac{1}{2}h_i} (\sigma_{x,i} \varepsilon_{x,i} + \sigma_{y,i} \varepsilon_{y,i} + \tau_{xy,i} \gamma_{xy,i}) dz + \right. \\ & \left. + \int_{z_s - \frac{1}{2}h_s}^{z_s + \frac{1}{2}h_s} (\tau_{xz,s} \gamma_{xz,s} + \tau_{yz,s} \gamma_{yz,s}) dz \right] dx dy, \end{aligned} \quad (68)$$

in the form

$$\begin{aligned} \mathcal{U} = & \frac{1}{2} \iint_{\Omega} \left(N_x \bar{\varepsilon}_x + N_y \bar{\varepsilon}_y + N_{xy} \bar{\gamma}_{xy} + M_x^K \chi_x^K + M_y^K \chi_y^K + M_{xy}^K \chi_{xy}^K + \right. \\ & \left. + M_x^M \gamma_x^M + M_y^M \gamma_y^M + M_{xy}^M \gamma_{xy}^M + Q_x^M \gamma_{xz}^M + Q_y^M \gamma_{yz}^M \right) dx dy, \end{aligned} \quad (69)$$

thus obtaining the following top-tier (two-dimensional) constitutive equations:

(i) Membrane forces:

$$N_x = \sum_{i=1}^2 \frac{E_i h_i}{1-\nu_i^2} \bar{\varepsilon}_x + \sum_{i=1}^2 \frac{z_i E_i h_i}{1-\nu_i^2} \chi_x^M + \sum_{i=1}^2 \frac{\nu_i E_i h_i}{1-\nu_i^2} \bar{\varepsilon}_y + \sum_{i=1}^2 \frac{z_i \nu_i E_i h_i}{1-\nu_i^2} \chi_y^M \quad (70)$$

$$N_y = \sum_{i=1}^2 \frac{E_i h_i}{1-\nu_i^2} \bar{\varepsilon}_y + \sum_{i=1}^2 \frac{z_i E_i h_i}{1-\nu_i^2} \chi_y^M + \sum_{i=1}^2 \frac{\nu_i E_i h_i}{1-\nu_i^2} \bar{\varepsilon}_x + \sum_{i=1}^2 \frac{z_i \nu_i E_i h_i}{1-\nu_i^2} \chi_x^M \quad (71)$$

$$N_{xy} = \sum_{i=1}^2 \frac{E_i h_i}{2(1+\nu_i)} \bar{\gamma}_{xy} + \sum_{i=1}^2 \frac{z_i E_i h_i}{2(1+\nu_i)} \chi_{xy}^M; \quad (72)$$

(ii) ‘‘Kirchhoff’’ bending and twisting moments:

$$M_x^K = \sum_{i=1}^2 \frac{E_i h_i^3}{12(1-\nu_i^2)} \chi_x^K + \sum_{i=1}^2 \frac{\nu_i E_i h_i^3}{12(1-\nu_i^2)} \chi_y^K \quad (73)$$

$$M_y^K = \sum_{i=1}^2 \frac{E_i h_i^3}{12(1-\nu_i^2)} \chi_y^K + \sum_{i=1}^2 \frac{\nu_i E_i h_i^3}{12(1-\nu_i^2)} \chi_x^K \quad (74)$$

$$M_{xy}^K = \sum_{i=1}^2 \frac{E_i h_i^3}{24(1+\nu_i)} \chi_{xy}^K; \quad (75)$$

(iii) ‘‘Mindlin’’ bending and twisting moments:

$$M_x^M = \sum_{i=1}^2 \frac{z_i E_i h_i}{1-\nu_i^2} \bar{\varepsilon}_x + \sum_{i=1}^2 \frac{z_i^2 E_i h_i}{1-\nu_i^2} \chi_x^M + \sum_{i=1}^2 \frac{z_i \nu_i E_i h_i}{1-\nu_i^2} \bar{\varepsilon}_y + \sum_{i=1}^2 \frac{z_i^2 \nu_i E_i h_i}{1-\nu_i^2} \chi_y^M \quad (76)$$

$$M_y^M = \sum_{i=1}^2 \frac{z_i E_i h_i}{1-\nu_i^2} \bar{\varepsilon}_y + \sum_{i=1}^2 \frac{z_i^2 E_i h_i}{1-\nu_i^2} \chi_y^M + \sum_{i=1}^2 \frac{z_i \nu_i E_i h_i}{1-\nu_i^2} \bar{\varepsilon}_x + \sum_{i=1}^2 \frac{z_i^2 \nu_i E_i h_i}{1-\nu_i^2} \chi_x^M \quad (77)$$

$$M_{xy}^M = \sum_{i=1}^2 \frac{z_i E_i h_i}{2(1+\nu_i)} \bar{\gamma}_{xy} + \sum_{i=1}^2 \frac{z_i^2 E_i h_i}{2(1+\nu_i)} \chi_{xy}^M; \quad (78)$$

(iv) ‘‘Mindlin’’ shear forces:

$$Q_x^M = G_{z,s} \frac{(z_2 - z_1)^2}{h_s} \gamma_{xz}^M \quad Q_y^M = G_{z,s} \frac{(z_2 - z_1)^2}{h_s} \gamma_{yz}^M. \quad (79)$$

It should be noticed that

$$N_x = \sum_{i=1}^2 N_{x,i} \quad N_y = \sum_{i=1}^2 N_{y,i} \quad N_{xy} = \sum_{i=1}^2 N_{xy,i} \quad (80)$$

$$M_x^K = \sum_{i=1}^2 M_{x,i} \quad M_y^K = \sum_{i=1}^2 M_{y,i} \quad M_{xy}^K = \sum_{i=1}^2 M_{xy,i} \quad (81)$$

$$M_x^M = \sum_{i=1}^2 z_i N_{x,i} \quad M_y^M = \sum_{i=1}^2 z_i N_{y,i} \quad M_{xy}^M = \sum_{i=1}^2 z_i N_{xy,i} \quad (82)$$

$$Q_x^M = \frac{z_2 - z_1}{h_s} Q_{x,s} \quad Q_y^M = \frac{z_2 - z_1}{h_s} Q_{y,s}. \quad (83)$$

2.5 Equilibrium

In keeping with our three-tier approach, we start by examining the equilibrium of the layers and of the interlayer considered in isolation.

Let the scalar fields $b_{x,i}$, $b_{y,i}$ and $b_{z,i}$, defined on $\bar{\Omega} \times [z_i - \frac{1}{2}h_i, z_i + \frac{1}{2}h_i]$, denote the Cartesian components of the body forces per unit volume that act upon layer i ($i = 1, 2$). They are assumed to be continuous, with $b_{x,i}$ (resp. $b_{y,i}$) also having a continuous partial derivative with respect to x (resp. y). Moreover, let the scalar fields $s_{x,i}^-$, $s_{y,i}^-$ and $s_{z,i}^-$ (resp. $s_{x,i}^+$, $s_{y,i}^+$ and $s_{z,i}^+$), defined on $\bar{\Omega}$, denote the Cartesian components of the surface tractions per unit area on the “top” face $\bar{\Omega} \times \{z_i - \frac{1}{2}h_i\}$ (resp. “bottom” face $\bar{\Omega} \times \{z_i + \frac{1}{2}h_i\}$) of layer i . Both $s_{x,i}^-$ and $s_{x,i}^+$ (resp. $s_{y,i}^-$ and $s_{y,i}^+$) are assumed to be continuous and to have a continuous partial derivative with respect to x (resp. y), while for $s_{z,i}^-$ and $s_{z,i}^+$ we only require continuity. These body forces and surface tractions are illustrated in Figure 2.3.⁸ For each individual layer i to be in equilibrium, it is necessary that the Cartesian components of the respective *symmetric* tensor field satisfy the Cauchy equations

$$\frac{\partial \sigma_{x,i}}{\partial x} + \frac{\partial \tau_{xy,i}}{\partial y} + \frac{\partial \tau_{xz,i}}{\partial z} + b_{x,i} = 0 \quad (84)$$

$$\frac{\partial \tau_{xy,i}}{\partial x} + \frac{\partial \sigma_{y,i}}{\partial y} + \frac{\partial \tau_{yz,i}}{\partial z} + b_{y,i} = 0 \quad (85)$$

$$\frac{\partial \tau_{xz,i}}{\partial x} + \frac{\partial \tau_{yz,i}}{\partial y} + \frac{\partial \sigma_{z,i}}{\partial z} + b_{z,i} = 0 \quad (86)$$

on $\Omega \times]z_i - \frac{1}{2}h_i, z_i + \frac{1}{2}h_i[$ and the traction boundary conditions

$$\tau_{xz,i}(x, y, z_i - \frac{1}{2}h_i) = -s_{x,i}^-(x, y) \quad \tau_{xz,i}(x, y, z_i + \frac{1}{2}h_i) = s_{x,i}^+(x, y) \quad (87)$$

$$\tau_{yz,i}(x, y, z_i - \frac{1}{2}h_i) = -s_{y,i}^-(x, y) \quad \tau_{yz,i}(x, y, z_i + \frac{1}{2}h_i) = s_{y,i}^+(x, y) \quad (88)$$

$$\sigma_{z,i}(x, y, z_i - \frac{1}{2}h_i) = -s_{z,i}^-(x, y) \quad \sigma_{z,i}(x, y, z_i + \frac{1}{2}h_i) = s_{z,i}^+(x, y) \quad (89)$$

on the end faces $\bar{\Omega} \times \{z_i \pm \frac{1}{2}h_i\}$.

⁸ With regard to the composite plate as a whole, $(s_{x,1}^-, s_{y,1}^-, s_{z,1}^-)$ and $(s_{x,2}^+, s_{y,2}^+, s_{z,2}^+)$ are external loads, while $(s_{x,1}^+, s_{y,1}^+, s_{z,1}^+)$ and $(s_{x,2}^-, s_{y,2}^-, s_{z,2}^-)$ are the internal contact forces exerted upon the layers across the layer/interlayer interface.

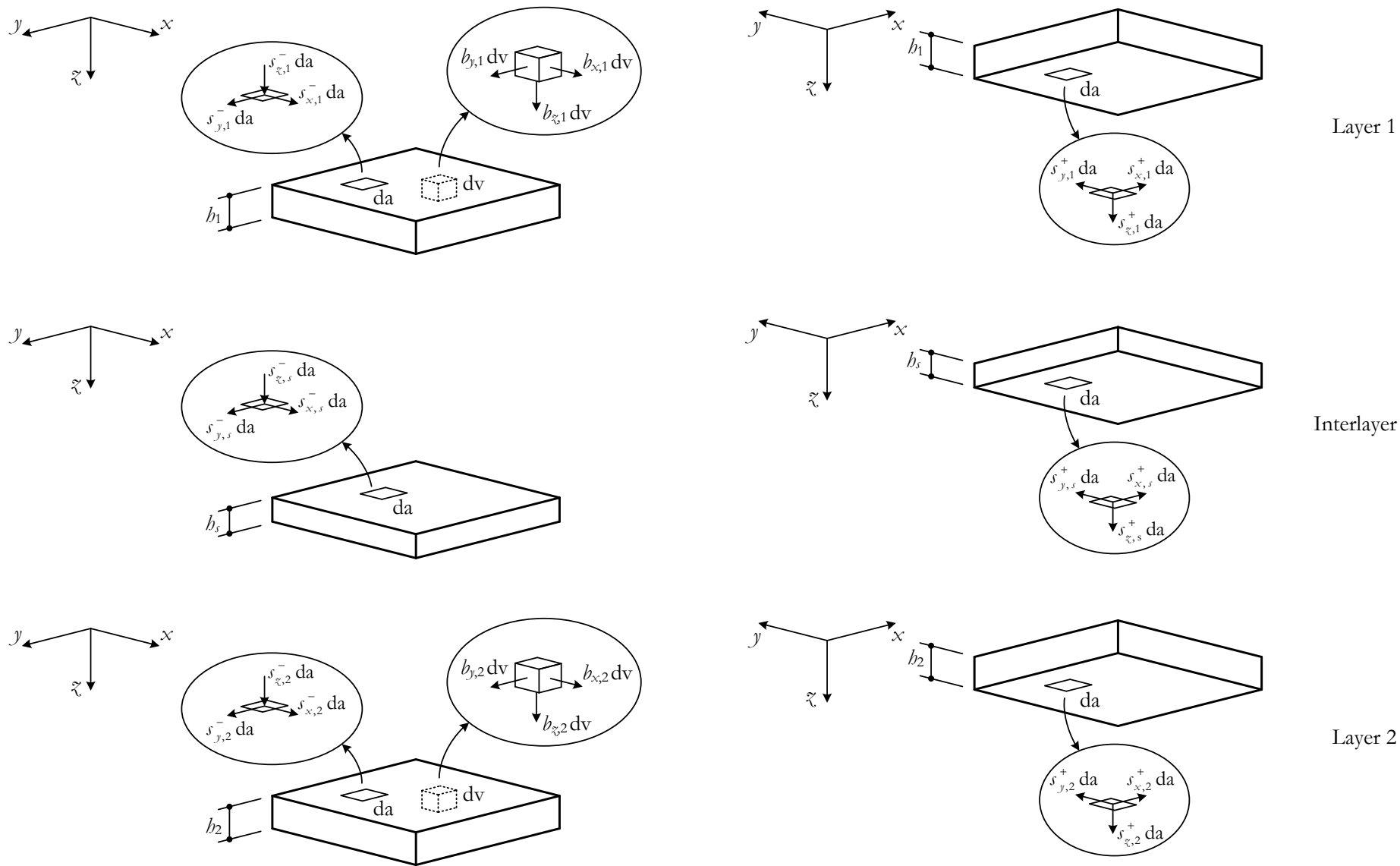


Figure 2.3: Surface tractions on the end faces and body forces for each of the two layers and for the interlayer

The interlayer is not subject to body forces (but body forces parallel to the z -axis could easily be included in the analysis) and we denote the surface tractions acting on its “top” and “bottom” faces by $(s_{x,s}^-, s_{y,s}^-, s_{z,s}^-)$ and $(s_{x,s}^+, s_{y,s}^+, s_{z,s}^+)$, respectively, with the same smoothness requirements as those specified above for the surface tractions on the end faces of the layers (Figure 2.3). By virtue of assumption A6 and the absence of body forces, the Cauchy equations for the interlayer reduce to

$$\frac{\partial \tau_{xz,s}}{\partial z} = 0 \quad (90)$$

$$\frac{\partial \tau_{yz,s}}{\partial z} = 0 \quad (91)$$

$$\frac{\partial \tau_{xz,s}}{\partial x} + \frac{\partial \tau_{yz,s}}{\partial y} + \frac{\partial \sigma_{z,s}}{\partial z} = 0. \quad (92)$$

They are subject to the traction boundary conditions

$$\tau_{xz,s}(x, y, z_s - \frac{1}{2}h_s) = -s_{x,s}^-(x, y) \quad \tau_{xz,s}(x, y, z_s + \frac{1}{2}h_s) = s_{x,s}^+(x, y) \quad (93)$$

$$\tau_{yz,s}(x, y, z_s - \frac{1}{2}h_s) = -s_{y,s}^-(x, y) \quad \tau_{yz,s}(x, y, z_s + \frac{1}{2}h_s) = s_{y,s}^+(x, y) \quad (94)$$

$$\sigma_{z,s}(x, y, z_s - \frac{1}{2}h_s) = -s_{z,s}^-(x, y) \quad \sigma_{z,s}(x, y, z_s + \frac{1}{2}h_s) = s_{z,s}^+(x, y) \quad (95)$$

on the “top” and “bottom” faces. The first two Cauchy equations assert that $\tau_{xz,s}$ and $\tau_{yz,s}$ are independent of z (*i.e.*, they are constant across the thickness of the interlayer), in agreement with our previous results (37)-(38) and (59). In particular, we must have

$$s_{x,s}^- + s_{x,s}^+ = 0 \quad s_{y,s}^- + s_{y,s}^+ = 0, \quad (96)$$

i.e., the surface tractions parallel to the x, y -plane on the “top” and “bottom” faces of the interlayer are symmetrical.

Let us now move up the ladder to the intermediate tier of the hierarchy and establish the equilibrium equations for each plate-like layer in terms of the respective through-the-thickness

stress resultants (Figure 2.4) – the membrane forces $N_{x,i} = \int_{z_i - \frac{1}{2}h_i}^{z_i + \frac{1}{2}h_i} \sigma_{x,i} dz$, $N_{y,i} = \int_{z_i - \frac{1}{2}h_i}^{z_i + \frac{1}{2}h_i} \sigma_{y,i} dz$ and $N_{xy,i} = \int_{z_i - \frac{1}{2}h_i}^{z_i + \frac{1}{2}h_i} \tau_{xy,i} dz$, the bending moments $M_{x,i} = \int_{z_i - \frac{1}{2}h_i}^{z_i + \frac{1}{2}h_i} (z - z_i) \sigma_{x,i} dz$

and $M_{y,i} = \int_{z_i - \frac{1}{2}h_i}^{z_i + \frac{1}{2}h_i} (z - z_i)\sigma_{y,i} dz$, the twisting moment $M_{xy,i} = \int_{z_i - \frac{1}{2}h_i}^{z_i + \frac{1}{2}h_i} (z - z_i)\tau_{xy,i} dz$ and the transverse shear forces $Q_{x,i} = \int_{z_i - \frac{1}{2}h_i}^{z_i + \frac{1}{2}h_i} \tau_{xz,i} dz$ and $Q_{y,i} = \int_{z_i - \frac{1}{2}h_i}^{z_i + \frac{1}{2}h_i} \tau_{yz,i} dz$ (the reactive stress fields $\tau_{xz,i}$ and $\tau_{yz,i}$ on each layer i are defined explicitly in Appendix 2).

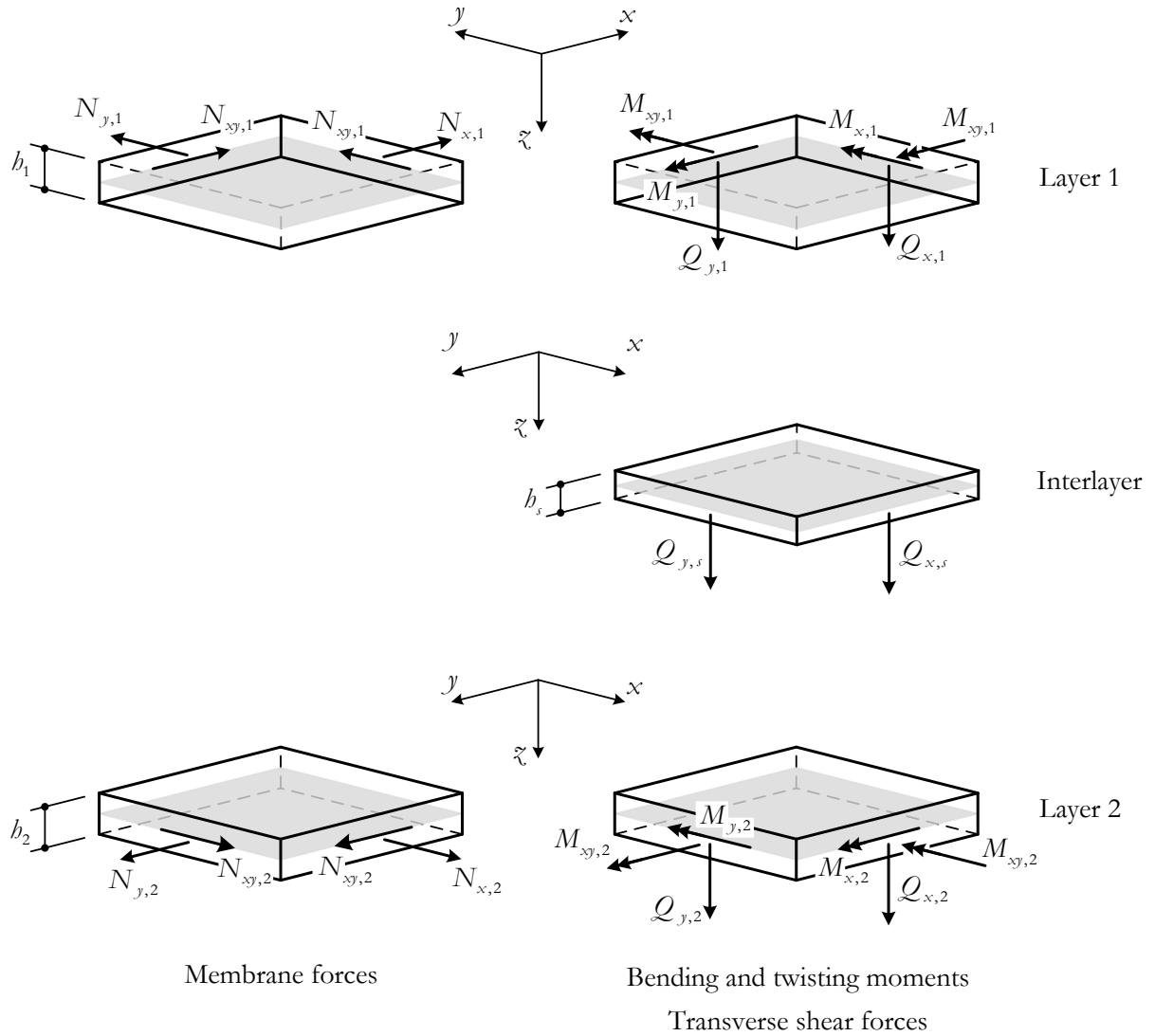


Figure 2.4: Through-the-thickness stress resultants on each layer and on the interlayer

If one takes (87)-(89) into consideration and appeals to Leibniz rule (*e.g.*, Bartle, 1976, th. 31.7), then the integration of equations (84)-(86) over the thickness of each layer yields three equilibrium equations on Ω per layer:

$$\frac{\partial N_{x,i}}{\partial x} + \frac{\partial N_{xy,i}}{\partial y} + q_{x,i} = 0 \quad (97)$$

$$\frac{\partial N_{xy,i}}{\partial x} + \frac{\partial N_{y,i}}{\partial y} + q_{y,i} = 0 \quad (98)$$

$$\frac{\partial Q_{x,i}}{\partial x} + \frac{\partial Q_{y,i}}{\partial y} + q_{z,i} = 0, \quad (99)$$

where

$$q_{x,i}(x, y) = s_{x,i}^- + s_{x,i}^+ + \int_{z_i - \frac{1}{2}h_i}^{z_i + \frac{1}{2}h_i} b_{x,i} dz \quad (100)$$

$$q_{y,i}(x, y) = s_{y,i}^- + s_{y,i}^+ + \int_{z_i - \frac{1}{2}h_i}^{z_i + \frac{1}{2}h_i} b_{y,i} dz \quad (101)$$

$$q_{z,i}(x, y) = s_{z,i}^- + s_{z,i}^+ + \int_{z_i - \frac{1}{2}h_i}^{z_i + \frac{1}{2}h_i} b_{z,i} dz \quad (102)$$

represent the Cartesian components of the resultant force distribution applied to layer i , defined per unit area of Ω . These differential equations constitute a local two-dimensional statement of translational equilibrium for each layer.

Similarly, if one multiplies equations (84)-(85) by $(z - z_i)$ and then integrates over the thickness of each layer, one obtains two further equilibrium equations on Ω per layer:

$$\frac{\partial M_{x,i}}{\partial x} + \frac{\partial M_{xy,i}}{\partial y} - Q_{x,i} + m_{x,i} = 0 \quad (103)$$

$$\frac{\partial M_{xy,i}}{\partial x} + \frac{\partial M_{y,i}}{\partial y} - Q_{y,i} + m_{y,i} = 0, \quad (104)$$

where

$$m_{x,i}(x, y) = \frac{h_i}{2} (s_{x,i}^+ - s_{x,i}^-) + \int_{z_i - \frac{1}{2}h_i}^{z_i + \frac{1}{2}h_i} (z - z_i) b_{x,i} dz \quad (105)$$

$$m_{y,i}(x, y) = \frac{h_i}{2} (s_{y,i}^+ - s_{y,i}^-) + \int_{z_i - \frac{1}{2}h_i}^{z_i + \frac{1}{2}h_i} (z - z_i) b_{y,i} dz. \quad (106)$$

Equations (103) and (104) are a local two-dimensional statement of rotational equilibrium for each layer.

An immediate consequence of (99) and (103)-(104) is that

$$\frac{\partial^2 M_{x,i}}{\partial x^2} + 2 \frac{\partial^2 M_{xy,i}}{\partial x \partial y} + \frac{\partial^2 M_{y,i}}{\partial y^2} + q_{z,i} + \frac{\partial m_{x,i}}{\partial x} + \frac{\partial m_{y,i}}{\partial y} = 0 \quad (107)$$

must hold on Ω .

We can apply a similar line of reasoning to the interlayer and thereby obtain, in addition to (96), the following two-dimensional equilibrium conditions in terms of the transverse shear

forces $Q_{x,s} = \int_{z_s - \frac{1}{2}h_s}^{z_s + \frac{1}{2}h_s} \tau_{xz,s} dz$ and $Q_{y,s} = \int_{z_s - \frac{1}{2}h_s}^{z_s + \frac{1}{2}h_s} \tau_{yz,s} dz$:

$$\frac{\partial Q_{x,s}}{\partial x} + \frac{\partial Q_{y,s}}{\partial y} + q_{z,s} = 0 \quad (108)$$

$$m_{x,s} - Q_{x,s} = 0 \quad (109)$$

$$m_{y,s} - Q_{y,s} = 0, \quad (110)$$

where

$$q_{z,s}(x, y) = s_{z,s}^- + s_{z,s}^+ \quad (111)$$

$$m_{x,s}(x, y) = \frac{h_s}{2} (s_{x,s}^+ - s_{x,s}^-) \quad (112)$$

$$m_{y,s}(x, y) = \frac{h_s}{2} (s_{y,s}^+ - s_{y,s}^-). \quad (113)$$

Plugging (109)-(110) into (108), we get

$$\frac{\partial m_{x,s}}{\partial x} + \frac{\partial m_{y,s}}{\partial y} + q_{z,s} = 0. \quad (114)$$

To reach the upper tier of the hierarchy, the next step is to impose, across each layer/interlayer interface, the stress continuity conditions

$$\tau_{xz,i} \left(x, y, z_i + (-1)^{i+1} \frac{1}{2} h_i \right) = \tau_{xz,s} \left(x, y, z_s + (-1)^i \frac{1}{2} h_s \right) \quad (115)$$

$$\tau_{yz,i} \left(x, y, z_i + (-1)^{i+1} \frac{1}{2} h_i \right) = \tau_{yz,s} \left(x, y, z_s + (-1)^i \frac{1}{2} h_s \right) \quad (116)$$

$$\sigma_{z,i} \left(x, y, z_i + (-1)^{i+1} \frac{1}{2} h_i \right) = \sigma_{z,s} \left(x, y, z_s + (-1)^i \frac{1}{2} h_s \right), \quad (x, y) \in \bar{\Omega}, \quad i = 1, 2, \quad (117)$$

which are equivalent to

$$s_{x,1}^+ = -s_{x,s}^- \quad s_{x,s}^+ = -s_{x,2}^- \quad (118)$$

$$s_{y,1}^+ = -s_{y,s}^- \quad s_{y,s}^+ = -s_{y,2}^- \quad (119)$$

$$s_{z,1}^+ = -s_{z,s}^- \quad s_{z,s}^+ = -s_{z,2}^- \quad (120)$$

From (118)-(119) and (96) we find that

$$s_{x,1}^+ = -s_{x,2}^- \quad s_{y,1}^+ = -s_{y,2}^- \quad (121)$$

Then, in view of (80), it follows from equations (97) and (98), by direct summation over $i = 1,2$, that

$$\frac{\partial N_x}{\partial x} + \frac{\partial N_{xy}}{\partial y} + q_x = 0 \quad (122)$$

$$\frac{\partial N_{xy}}{\partial x} + \frac{\partial N_y}{\partial y} + q_y = 0, \quad (123)$$

where

$$q_x(x, y) = \sum_{i=1}^2 q_{x,i} = s_{x,1}^- + s_{x,2}^+ + \sum_{i=1}^2 \int_{z_i - \frac{1}{2}h_i}^{z_i + \frac{1}{2}h_i} b_{x,i} dz \quad (124)$$

$$q_y(x, y) = \sum_{i=1}^2 q_{y,i} = s_{y,1}^- + s_{y,2}^+ + \sum_{i=1}^2 \int_{z_i - \frac{1}{2}h_i}^{z_i + \frac{1}{2}h_i} b_{y,i} dz \quad (125)$$

represent the resultant external force distribution, in the x - and y -directions, applied to the composite plate (excluding its lateral surface $\Gamma \times]z_1 - \frac{1}{2}h_1, z_2 + \frac{1}{2}h_2[$) and defined per unit area of Ω . Similarly, the direct summation of equations (107) (over $i = 1,2$) and (114) yields

$$\frac{\partial^2 M_x^K}{\partial x^2} + 2 \frac{\partial^2 M_{xy}^K}{\partial x \partial y} + \frac{\partial^2 M_y^K}{\partial y^2} + \frac{\partial Q_x^M}{\partial x} + \frac{\partial Q_y^M}{\partial y} + q_z + \frac{\partial m_x^K}{\partial x} + \frac{\partial m_y^K}{\partial y} = 0, \quad (126)$$

where

$$q_z(x, y) = \sum_{i=1}^2 q_{z,i} + q_{z,s} = s_{z,1}^- + s_{z,2}^+ + \sum_{i=1}^2 \int_{z_i - \frac{1}{2}h_i}^{z_i + \frac{1}{2}h_i} b_{z,i} dz \quad (127)$$

$$m_x^K(x, y) = -\frac{h_1}{2} s_{x,1}^- + \frac{h_2}{2} s_{x,2}^+ + \sum_{i=1}^2 \int_{z_i - \frac{1}{2}h_i}^{z_i + \frac{1}{2}h_i} (z - z_i) b_{x,i} dz \quad (128)$$

$$m_y^K(x, y) = -\frac{h_1}{2} s_{y,1}^- + \frac{h_2}{2} s_{y,2}^+ + \sum_{i=1}^2 \int_{z_i - \frac{1}{2}h_i}^{z_i + \frac{1}{2}h_i} (z - z_i) b_{y,i} dz. \quad (129)$$

To obtain (126), we have also used the identities

$$\sum_{i=1}^2 m_{x,i} + m_{x,s} = m_x^K + \frac{z_2 - z_1}{h_s} Q_{x,s} = m_x^K + Q_x^M \quad (130)$$

$$\sum_{i=1}^2 m_{y,i} + m_{y,s} = m_y^K + \frac{z_2 - z_1}{h_s} Q_{y,s} = m_y^K + Q_y^M. \quad (131)$$

In addition, these identities, together with equations (103)-(104) and (109)-(110), enable us to recognise that the total transverse shear forces in the layered plate,

$$Q_x(x, y) = Q_{x,1} + Q_{x,s} + Q_{x,2} = \underbrace{\frac{\partial M_x^K}{\partial x} + \frac{\partial M_{xy}^K}{\partial y} + m_x^K}_{Q_x^{(r)}} + \underbrace{Q_x^M}_{Q_x^{(a)}} \quad (132)$$

$$Q_y(x, y) = Q_{y,1} + Q_{y,s} + Q_{y,2} = \underbrace{\frac{\partial M_{xy}^K}{\partial x} + \frac{\partial M_y^K}{\partial y} + m_y^K}_{Q_y^{(r)}} + \underbrace{Q_y^M}_{Q_y^{(a)}}, \quad (133)$$

are partly active ($Q_x^{(a)}$ and $Q_y^{(a)}$), to the extent that they are associated with the transverse shearing deformation of the interlayer, and partly reactive ($Q_x^{(r)}$ and $Q_y^{(r)}$), by virtue of the Kirchhoff internal constraint A3.1.

The remaining two top-tier equilibrium equations follow from (97)-(98) through multiplication by z_i and summation over $i = 1, 2$. In view of (82)-(83), (96), (100)-(101), (109)-(110), (112)-(113) and (118)-(119), one gets

$$\frac{\partial M_x^M}{\partial x} + \frac{\partial M_{xy}^M}{\partial y} - Q_x^M + m_x^M = 0 \quad (134)$$

$$\frac{\partial M_{xy}^M}{\partial x} + \frac{\partial M_y^M}{\partial y} - Q_y^M + m_y^M = 0, \quad (135)$$

where

$$m_x^M(x, y) = z_1 s_{x,1}^- + z_2 s_{x,2}^+ + \sum_{i=1}^2 z_i \int_{z_i - \frac{1}{2}h_i}^{z_i + \frac{1}{2}h_i} b_{x,i} dz \quad (136)$$

$$m_y^M(x, y) = z_1 s_{y,1}^- + z_2 s_{y,2}^+ + \sum_{i=1}^2 z_i \int_{z_i - \frac{1}{2}h_i}^{z_i + \frac{1}{2}h_i} b_{y,i} dz. \quad (137)$$

It should be noticed that

$$m_x^K + m_x^M = \left(z_1 - \frac{h_1}{2}\right) s_{x,1}^- + \left(z_2 + \frac{h_2}{2}\right) s_{x,2}^+ + \sum_{i=1}^2 \int_{z_i - \frac{1}{2}h_i}^{z_i + \frac{1}{2}h_i} z b_{x,i} dz \quad (138)$$

$$m_y^K + m_y^M = \left(z_1 - \frac{h_1}{2}\right) s_{y,1}^- + \left(z_2 + \frac{h_2}{2}\right) s_{y,2}^+ + \sum_{i=1}^2 \int_{z_i - \frac{1}{2}h_i}^{z_i + \frac{1}{2}h_i} z b_{y,i} dz \quad (139)$$

represent the moment distribution, with respect to the plane $z = 0$, of the external forces applied to the composite plate (excluding its lateral surface $\Gamma \times]z_1 - \frac{1}{2}h_1, z_2 + \frac{1}{2}h_2[$), defined per unit area of Ω .

In the manner of Gjelsvik (1981, pp. 25-27), we refer to $q_x, q_y, q_z, m_x^K, m_y^K, m_x^M$ and m_y^M as plate loads.

2.6 The boundary value problem for the top-tier generalized displacements

Upon combining the strain-displacement relations (45) to (48), the constitutive equations (70) to (79) and the equilibrium conditions (122), (123), (126), (134) and (135), we obtain the governing field equations for the layered plate in terms of the 5 generalized displacement fields U, V, W, φ_x and φ_y (in equation (142), ∇^2 and ∇^4 denote the Laplace and biharmonic operators in the x, y -plane):

$$\begin{aligned} & \sum_{i=1}^2 \frac{E_i h_i}{1-\nu_i^2} \frac{\partial^2 U}{\partial x^2} + \sum_{i=1}^2 \frac{E_i h_i}{2(1+\nu_i)} \frac{\partial^2 U}{\partial y^2} + \sum_{i=1}^2 \frac{E_i h_i}{2(1-\nu_i)} \frac{\partial^2 V}{\partial x \partial y} - \sum_{i=1}^2 \frac{z_i E_i h_i}{1-\nu_i^2} \frac{\partial^2 \varphi_x}{\partial x^2} - \\ & - \sum_{i=1}^2 \frac{z_i E_i h_i}{2(1+\nu_i)} \frac{\partial^2 \varphi_x}{\partial y^2} - \sum_{i=1}^2 \frac{z_i E_i h_i}{2(1-\nu_i)} \frac{\partial^2 \varphi_y}{\partial x \partial y} + q_x = 0 \end{aligned} \quad (140)$$

$$\begin{aligned} & \sum_{i=1}^2 \frac{E_i h_i}{2(1-\nu_i)} \frac{\partial^2 U}{\partial x \partial y} + \sum_{i=1}^2 \frac{E_i h_i}{2(1+\nu_i)} \frac{\partial^2 V}{\partial x^2} + \sum_{i=1}^2 \frac{E_i h_i}{1-\nu_i^2} \frac{\partial^2 V}{\partial y^2} - \sum_{i=1}^2 \frac{z_i E_i h_i}{2(1-\nu_i)} \frac{\partial^2 \varphi_x}{\partial x \partial y} - \\ & - \sum_{i=1}^2 \frac{z_i E_i h_i}{2(1+\nu_i)} \frac{\partial^2 \varphi_y}{\partial x^2} - \sum_{i=1}^2 \frac{z_i E_i h_i}{1-\nu_i^2} \frac{\partial^2 \varphi_y}{\partial y^2} + q_y = 0 \end{aligned} \quad (141)$$

$$- \sum_{i=1}^2 \frac{E_i h_i^3}{12(1-\nu_i^2)} \nabla^4 W + G_{z,s} \frac{(z_2 - z_1)^2}{h_s} \left(\nabla^2 W - \frac{\partial \varphi_x}{\partial x} - \frac{\partial \varphi_y}{\partial y} \right) + q_z + \frac{\partial m_x^K}{\partial x} + \frac{\partial m_y^K}{\partial y} = 0 \quad (142)$$

$$\begin{aligned}
& \sum_{i=1}^2 \frac{z_i E_i h_i}{1-\nu_i^2} \frac{\partial^2 U}{\partial x^2} + \sum_{i=1}^2 \frac{z_i E_i h_i}{2(1+\nu_i)} \frac{\partial^2 U}{\partial y^2} + \sum_{i=1}^2 \frac{z_i E_i h_i}{2(1-\nu_i)} \frac{\partial^2 V}{\partial x \partial y} - G_{z,s} \frac{(z_2-z_1)^2}{h_s} \frac{\partial W}{\partial x} - \\
& - \sum_{i=1}^2 \frac{z_i^2 E_i h_i}{1-\nu_i^2} \frac{\partial^2 \varphi_x}{\partial x^2} - \sum_{i=1}^2 \frac{z_i^2 E_i h_i}{2(1+\nu_i)} \frac{\partial^2 \varphi_x}{\partial y^2} + G_{z,s} \frac{(z_2-z_1)^2}{h_s} \varphi_x - \\
& - \sum_{i=1}^2 \frac{z_i^2 E_i h_i}{2(1-\nu_i)} \frac{\partial^2 \varphi_y}{\partial x \partial y} + m_x^M = 0
\end{aligned} \tag{143}$$

$$\begin{aligned}
& \sum_{i=1}^2 \frac{z_i E_i h_i}{2(1-\nu_i)} \frac{\partial^2 U}{\partial x \partial y} + \sum_{i=1}^2 \frac{z_i E_i h_i}{2(1+\nu_i)} \frac{\partial^2 V}{\partial x^2} + \sum_{i=1}^2 \frac{z_i E_i h_i}{1-\nu_i^2} \frac{\partial^2 V}{\partial y^2} - G_{z,s} \frac{(z_2-z_1)^2}{h_s} \frac{\partial W}{\partial y} - \\
& - \sum_{i=1}^2 \frac{z_i^2 E_i h_i}{2(1-\nu_i)} \frac{\partial^2 \varphi_x}{\partial x \partial y} - \sum_{i=1}^2 \frac{z_i^2 E_i h_i}{2(1+\nu_i)} \frac{\partial^2 \varphi_y}{\partial x^2} - \sum_{i=1}^2 \frac{z_i^2 E_i h_i}{1-\nu_i^2} \frac{\partial^2 \varphi_y}{\partial y^2} + \\
& + G_{z,s} \frac{(z_2-z_1)^2}{h_s} \varphi_y + m_y^M = 0.
\end{aligned} \tag{144}$$

There are six boundary conditions to be prescribed on Γ (or on each element of a partition of Γ) – one more than in the theory of Mindlin and two more than in the theory of Kirchhoff. One possibility is to prescribe (the reader should regard the generalized stresses as written in terms of generalized displacements)

- (i) either U or $N_x n_x + N_{xy} n_y$;
- (ii) either V or $N_{xy} n_x + N_y n_y$;
- (iii) either W or $Q_n + \frac{\partial M_{nt}^K}{\partial t}$, where

$$Q_n = Q_x n_x + Q_y n_y \tag{145}$$

$$M_{nt}^K = M_{xy}^K (n_x^2 - n_y^2) + (M_y^K - M_x^K) n_x n_y \tag{146}$$

and

$$\frac{\partial}{\partial t} = -n_y \frac{\partial}{\partial x} + n_x \frac{\partial}{\partial y} \tag{147}$$

is the tangential derivative operator along Γ ;

- (iv) either $\frac{\partial W}{\partial n}$ or M_n^K , where

$$M_n^K = M_x^K n_x^2 + M_y^K n_y^2 + 2M_{xy}^K n_x n_y \tag{148}$$

and

$$\frac{\partial}{\partial n} = n_x \frac{\partial}{\partial x} + n_y \frac{\partial}{\partial y} \quad (149)$$

is the outer normal derivative operator along Γ ;

(v) either φ_x or $M_x^M n_x + M_{xy}^M n_y$;

(vi) either φ_y or $M_{xy}^M n_x + M_y^M n_y$.

The boundary value problem is greatly simplified if $\nu_1 = \nu_2$ and the plane $z = 0$ is chosen so that $\sum_{i=1}^2 z_i E_i h_i = 0$. Indeed, under these circumstances, the generalized displacements U and V become uncoupled from W , φ_x and φ_y – in other words, the boundary value problem splits into a “membrane problem” and a “bending problem”, independent of each other.

3 AN ILLUSTRATIVE PROBLEM WITH CLOSED-FORM EXACT SOLUTION AND ITS GENERALIZATION

Consider a thin two-layer rectangular plate with dimensions a and b . The chosen Cartesian reference system is shown in Figure 3.1 and is such that $\sum_{i=1}^2 z_i E_i h_i = 0$. Regarding the material properties, it is assumed that $\nu_1 = \nu_2 = \nu$. Our task is to solve the “bending problem” for this plate when a transverse surface load

$$s_{z,1}^-(x, y) = q_0 \sin\left(\frac{\pi x}{a}\right) \sin\left(\frac{\pi y}{b}\right) \quad (150)$$

is applied to its “top” face. The boundary conditions are also indicated in Figure 3.1.

Since $W = 0$ along all four edges, it follows that $\frac{\partial^2 W}{\partial x^2} = 0$ along the edges parallel to the x -axis and $\frac{\partial^2 W}{\partial y^2} = 0$ along the edges parallel to the y -axis. Similarly, the condition $\varphi_x = 0$ (resp. $\varphi_y = 0$) along the edges parallel to the x -axis (resp. the y -axis) causes the vanishing of

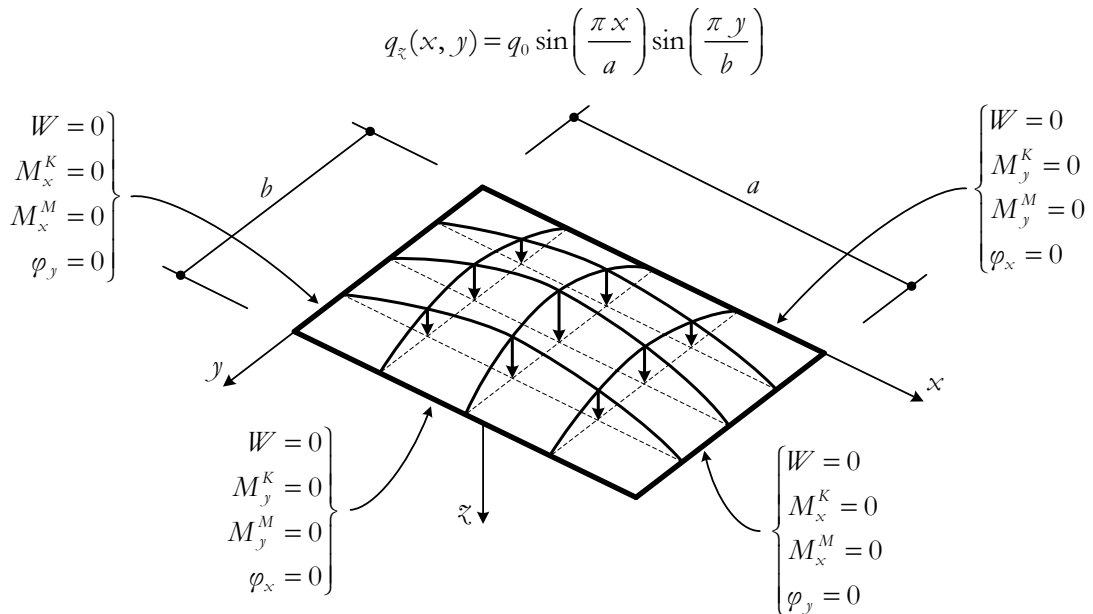


Figure 3.1: Illustrative problem – Geometry, loading and boundary conditions

$\frac{\partial \varphi_x}{\partial x}$ (resp. $\frac{\partial \varphi_y}{\partial y}$) along those edges as well. Accordingly, the moment boundary conditions in Figure 3.1 are equivalent to

$$\frac{\partial^2 W}{\partial x^2}(0, y) = \frac{\partial^2 W}{\partial x^2}(a, y) = 0 \quad \frac{\partial^2 W}{\partial y^2}(x, 0) = \frac{\partial^2 W}{\partial y^2}(x, b) = 0 \quad (151)$$

$$\frac{\partial \varphi_x}{\partial x}(0, y) = \frac{\partial \varphi_x}{\partial x}(a, y) = 0 \quad \frac{\partial \varphi_y}{\partial y}(x, 0) = \frac{\partial \varphi_y}{\partial y}(x, b) = 0. \quad (152)$$

A trial solution of the form

$$W(x, y) = W_0 \sin\left(\frac{\pi x}{a}\right) \sin\left(\frac{\pi y}{b}\right) \quad (153)$$

$$\varphi_x(x, y) = X_0 \cos\left(\frac{\pi x}{a}\right) \sin\left(\frac{\pi y}{b}\right) \quad (154)$$

$$\varphi_y(x, y) = Y_0 \sin\left(\frac{\pi x}{a}\right) \cos\left(\frac{\pi y}{b}\right) \quad (155)$$

satisfies all boundary conditions. We must now examine whether it is possible to find real constants W_0 , X_0 and Y_0 so as to satisfy the field equations

$$-\frac{\sum_{i=1}^2 E_i h_i^3}{12(1-\nu^2)} \nabla^4 W + G_{z,s} \frac{(z_2 - z_1)^2}{h_s} \left(\nabla^2 W - \frac{\partial \varphi_x}{\partial x} - \frac{\partial \varphi_y}{\partial y} \right) + q_z = 0 \quad (156)$$

$$G_{z,s} \frac{(z_2 - z_1)^2}{h_s} \left(\frac{\partial W}{\partial x} - \varphi_x \right) + \frac{\sum_{i=1}^2 z_i^2 E_i h_i}{1-\nu^2} \left(\frac{\partial^2 \varphi_x}{\partial x^2} + \frac{1-\nu}{2} \frac{\partial^2 \varphi_x}{\partial y^2} + \frac{1+\nu}{2} \frac{\partial^2 \varphi_y}{\partial x \partial y} \right) = 0 \quad (157)$$

$$G_{z,s} \frac{(z_2 - z_1)^2}{h_s} \left(\frac{\partial W}{\partial y} - \varphi_y \right) + \frac{\sum_{i=1}^2 z_i^2 E_i h_i}{1-\nu^2} \left(\frac{1+\nu}{2} \frac{\partial^2 \varphi_x}{\partial x \partial y} + \frac{1-\nu}{2} \frac{\partial^2 \varphi_y}{\partial x^2} + \frac{\partial^2 \varphi_y}{\partial y^2} \right) = 0, \quad (158)$$

with $q_z = s_{z,1}^-$, everywhere on $]0, a[\times]0, b[$. To do so, we start by rewriting these field equations in non-dimensional form on a fixed reference domain, independent of the plate dimensions a and b . Consider the change of independent variables

$$x \mapsto \xi = \frac{x}{a} \quad y \mapsto \eta = \frac{y}{b} \quad (159)$$

and define new dependent variables

$$\bar{W}(\xi, \eta) = \frac{1}{a} W(\xi a, \eta b) = \frac{W_0}{a} \sin(\pi \xi) \sin(\pi \eta) \quad (160)$$

$$\bar{\varphi}_x(\xi, \eta) = \varphi_x(\xi a, \eta b) = X_0 \cos(\pi \xi) \sin(\pi \eta) \quad (161)$$

$$\bar{\varphi}_y(\xi, \eta) = \varphi_y(\xi a, \eta b) = Y_0 \sin(\pi \xi) \cos(\pi \eta), \quad (162)$$

whose domain is the unit square $[0, 1] \times [0, 1]$. Given non-negative integers m and n , the chain rule yields

$$\frac{\partial^{m+n} W}{\partial x^m \partial y^n}(x, y) = \frac{1}{a^{m-1} b^n} \frac{\partial^{m+n} \bar{W}}{\partial \xi^m \partial \eta^n}(\xi, \eta) = \frac{\pi^{m+n}}{a^m b^n} W_0 \sin\left(\pi\xi + m\frac{\pi}{2}\right) \sin\left(\pi\eta + n\frac{\pi}{2}\right) \quad (163)$$

$$\frac{\partial^{m+n} \varphi_x}{\partial x^m \partial y^n}(x, y) = \frac{1}{a^m b^n} \frac{\partial^{m+n} \bar{\varphi}_x}{\partial \xi^m \partial \eta^n}(\xi, \eta) = \frac{\pi^{m+n}}{a^m b^n} X_0 \cos\left(\pi\xi + m\frac{\pi}{2}\right) \sin\left(\pi\eta + n\frac{\pi}{2}\right) \quad (164)$$

$$\frac{\partial^{m+n} \varphi_y}{\partial x^m \partial y^n}(x, y) = \frac{1}{a^m b^n} \frac{\partial^{m+n} \bar{\varphi}_y}{\partial \xi^m \partial \eta^n}(\xi, \eta) = \frac{\pi^{m+n}}{a^m b^n} Y_0 \sin\left(\pi\xi + m\frac{\pi}{2}\right) \cos\left(\pi\eta + n\frac{\pi}{2}\right) \quad (165)$$

(the zeroth-order derivative means the function itself). Inserting these results into the differential equations (156) to (158) and introducing the non-dimensional ratios:

$$\rho = \frac{a}{b} \quad (166)$$

$$\alpha = \frac{12(1-\nu^2)G_{z,s} a^2 (z_2 - z_1)^2}{h_s \sum_{i=1}^2 E_i h_i^3} \quad (167)$$

$$\beta = \frac{12 \sum_{i=1}^2 z_i^2 E_i h_i}{\sum_{i=1}^2 E_i h_i^3} \quad (168)$$

$$\lambda = \frac{12(1-\nu^2)a^3 q_0}{\sum_{i=1}^2 E_i h_i^3}, \quad (169)$$

we obtain

$$\left\{ -\pi^2(1 + \rho^2)[\alpha + \pi^2(1 + \rho^2)] \frac{W_0}{a} + \pi\alpha(X_0 + \rho Y_0) + \lambda \right\} \sin(\pi\xi) \sin(\pi\eta) = 0 \quad (170)$$

$$\left\{ \pi\alpha \frac{W_0}{a} - \left[\alpha + \pi^2\beta \left(1 + \frac{1-\nu}{2} \rho^2 \right) \right] X_0 - \pi^2\beta\rho \frac{1+\nu}{2} Y_0 \right\} \cos(\pi\xi) \sin(\pi\eta) = 0 \quad (171)$$

$$\left\{ \pi\alpha\rho \frac{W_0}{a} - \pi^2\beta\rho \frac{1+\nu}{2} X_0 - \left[\alpha + \pi^2\beta \left(\frac{1-\nu}{2} + \rho^2 \right) \right] Y_0 \right\} \sin(\pi\xi) \cos(\pi\eta) = 0. \quad (172)$$

Since these equalities must hold for every $(\xi, \eta) \in]0,1[\times]0,1[$, it follows that

$$-\pi^2(1 + \rho^2)[\alpha + \pi^2(1 + \rho^2)] \frac{W_0}{a} + \pi\alpha(X_0 + \rho Y_0) + \lambda = 0 \quad (173)$$

$$\pi\alpha \frac{W_0}{a} - \left[\alpha + \pi^2\beta \left(1 + \frac{1-\nu}{2} \rho^2 \right) \right] X_0 - \pi^2\beta\rho \frac{1+\nu}{2} Y_0 = 0 \quad (174)$$

$$\pi\alpha\rho \frac{W_0}{a} - \pi^2\beta\rho \frac{1+\nu}{2} X_0 - \left[\alpha + \pi^2\beta \left(\frac{1-\nu}{2} + \rho^2 \right) \right] Y_0 = 0 \quad (175)$$

and from this linear algebraic system we find

$$\frac{W_0}{a} = \frac{\alpha + \pi^2 \beta (1 + \rho^2)}{\pi^4 (1 + \rho^2)^2 [\alpha (1 + \beta) + \pi^2 \beta (1 + \rho^2)]} \lambda \quad (176)$$

$$X_0 = \frac{\alpha}{\pi^3 (1 + \rho^2)^2 [\alpha (1 + \beta) + \pi^2 \beta (1 + \rho^2)]} \lambda \quad (177)$$

$$Y_0 = \frac{\alpha \rho}{\pi^3 (1 + \rho^2)^2 [\alpha (1 + \beta) + \pi^2 \beta (1 + \rho^2)]} \lambda = \rho X_0. \quad (178)$$

Now that the upper-tier generalized displacements are known, all other quantities of interest can be found by differentiation, irrespective of their position in the three-tier hierarchy that we have established at the outset of this work. For instance, the top-tier active generalized stress distributions are given by:

(i) ‘‘Kirchhoff’’ bending and twisting moments

$$M_x^K = -\frac{\sum_{i=1}^2 E_i h_i^3}{12(1-\nu^2)} \left(\frac{\partial^2 W}{\partial x^2} + \nu \frac{\partial^2 W}{\partial y^2} \right) = \frac{\pi^2 \sum_{i=1}^2 E_i h_i^3}{12(1-\nu^2)} \left(\frac{1}{a^2} + \frac{\nu}{b^2} \right) W_0 \sin\left(\frac{\pi x}{a}\right) \sin\left(\frac{\pi y}{b}\right) \quad (179)$$

$$M_y^K = -\frac{\sum_{i=1}^2 E_i h_i^3}{12(1-\nu^2)} \left(\nu \frac{\partial^2 W}{\partial x^2} + \frac{\partial^2 W}{\partial y^2} \right) = \frac{\pi^2 \sum_{i=1}^2 E_i h_i^3}{12(1-\nu^2)} \left(\frac{\nu}{a^2} + \frac{1}{b^2} \right) W_0 \sin\left(\frac{\pi x}{a}\right) \sin\left(\frac{\pi y}{b}\right) \quad (180)$$

$$M_{xy}^K = -\frac{\sum_{i=1}^2 E_i h_i^3}{12(1+\nu)} \frac{\partial^2 W}{\partial x \partial y} = -\frac{\pi^2 \sum_{i=1}^2 E_i h_i^3}{12(1+\nu)} \frac{W_0}{ab} \cos\left(\frac{\pi x}{a}\right) \cos\left(\frac{\pi y}{b}\right); \quad (181)$$

(ii) ‘‘Mindlin’’ bending and twisting moments

$$M_x^M = -\frac{\sum_{i=1}^2 z_i^2 E_i h_i}{1-\nu^2} \left(\frac{\partial \varphi_x}{\partial x} + \nu \frac{\partial \varphi_y}{\partial y} \right) = \frac{\pi \sum_{i=1}^2 z_i^2 E_i h_i}{1-\nu^2} \left(\frac{1}{a^2} + \frac{\nu}{b^2} \right) a X_0 \sin\left(\frac{\pi x}{a}\right) \sin\left(\frac{\pi y}{b}\right) \quad (182)$$

$$M_y^M = -\frac{\sum_{i=1}^2 z_i^2 E_i h_i}{1-\nu^2} \left(\nu \frac{\partial \varphi_x}{\partial x} + \frac{\partial \varphi_y}{\partial y} \right) = \frac{\pi \sum_{i=1}^2 z_i^2 E_i h_i}{1-\nu^2} \left(\frac{\nu}{a^2} + \frac{1}{b^2} \right) a X_0 \sin\left(\frac{\pi x}{a}\right) \sin\left(\frac{\pi y}{b}\right) \quad (183)$$

$$M_{xy}^M = -\frac{\sum_{i=1}^2 z_i^2 E_i h_i}{2(1+\nu)} \left(\frac{\partial \varphi_x}{\partial y} + \frac{\partial \varphi_y}{\partial x} \right) = -\frac{\pi \sum_{i=1}^2 z_i^2 E_i h_i}{1+\nu} \frac{X_0}{b} \cos\left(\frac{\pi x}{a}\right) \cos\left(\frac{\pi y}{b}\right); \quad (184)$$

(iii) ‘‘Mindlin’’ shear forces

$$Q_x^M = G_{z,s} \frac{(z_2 - z_1)^2}{h_s} \left(\frac{\partial W}{\partial x} - \varphi_x \right) = G_{z,s} \frac{(z_2 - z_1)^2}{h_s} \left(\frac{\pi}{a} W_0 - X_0 \right) \cos\left(\frac{\pi x}{a}\right) \sin\left(\frac{\pi y}{b}\right) \quad (185)$$

$$Q_y^M = G_{z,s} \frac{(z_2 - z_1)^2}{h_s} \left(\frac{\partial W}{\partial y} - \varphi_y \right) = G_{z,s} \frac{(z_2 - z_1)^2}{h_s} \left(\frac{\pi}{b} W_0 - Y_0 \right) \sin\left(\frac{\pi x}{a}\right) \cos\left(\frac{\pi y}{b}\right). \quad (186)$$

The shape of these distributions is shown qualitatively in Figures 3.2-3.5 under the assumption $q_0 > 0$ (hence $W_0 > 0$, $\frac{\pi}{a} W_0 > X_0 \geq 0$ and $\frac{\pi}{b} W_0 = \frac{\pi}{a} \rho W_0 > Y_0 \geq 0$) and, in the

case of Figure 3.2, also under the assumption $\nu > \max\left\{-\left(\frac{a}{b}\right)^2, -\left(\frac{b}{a}\right)^2\right\}$ (hence $\frac{1}{a^2} + \frac{\nu}{b^2} > 0$ and $\frac{\nu}{a^2} + \frac{1}{b^2} > 0$).

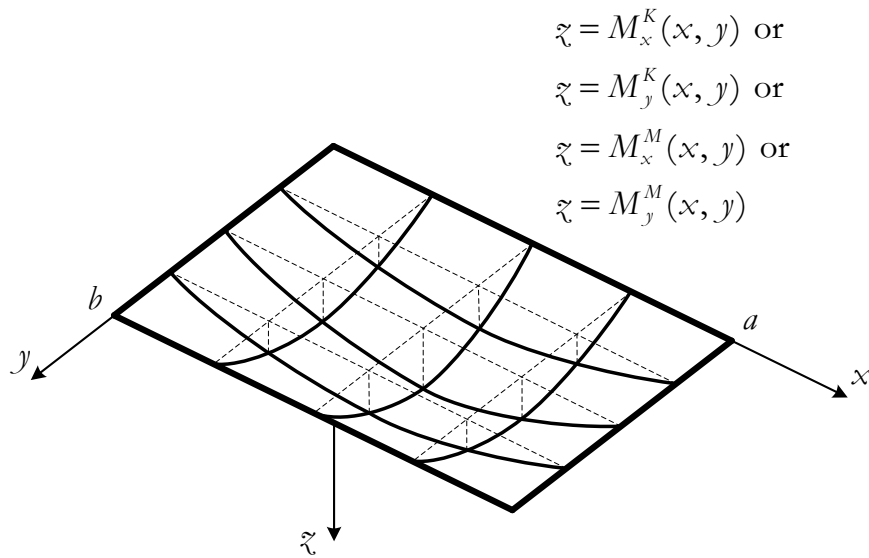


Figure 3.2: Illustrative problem – Qualitative shape of the distributions of “Kirchhoff” and “Mindlin” bending moments, assuming $q_0 > 0$ and $\nu > \max\left\{-\left(\frac{a}{b}\right)^2, -\left(\frac{b}{a}\right)^2\right\}$

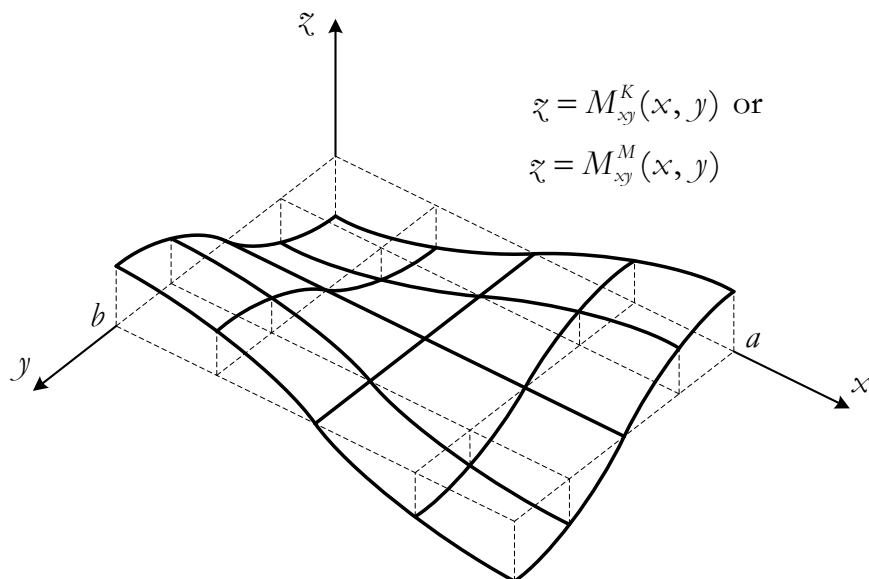


Figure 3.3: Illustrative problem – Qualitative shape of the distributions of “Kirchhoff” and “Mindlin” twisting moments, assuming $q_0 > 0$

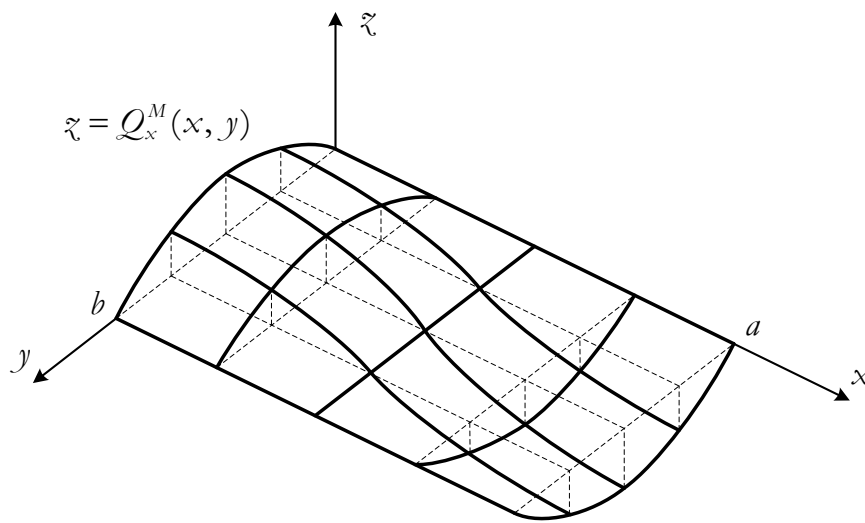


Figure 3.4: Illustrative problem – Qualitative shape of the distribution of “Mindlin” shear forces Q_x^M , assuming $q_0 > 0$

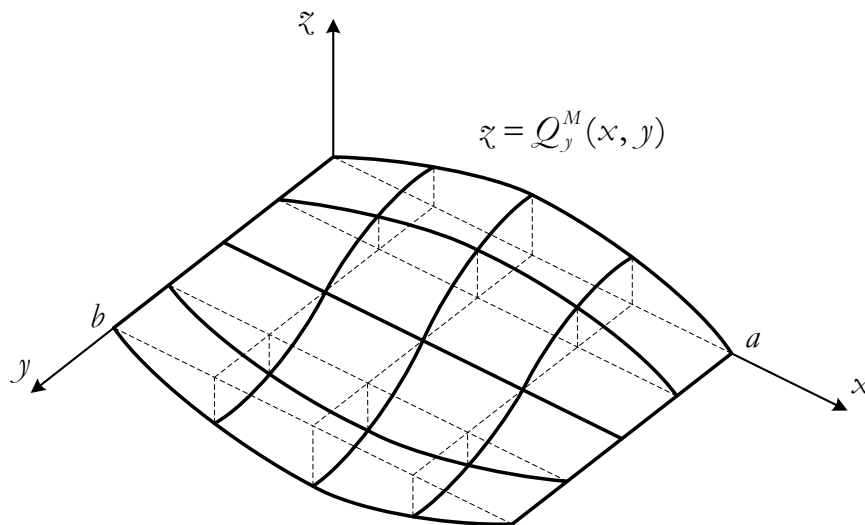


Figure 3.5: Illustrative problem – Qualitative shape of the distribution of “Mindlin” shear forces Q_y^M , assuming $q_0 > 0$

We shall now examine in some detail the “vertical” (*i.e.*, parallel to the z -axis) support reactions, whose determination is not without its subtleties. We have to take into account the total shear force and the “Kirchhoff” twisting moment distributions along the edges, but not the “Mindlin” twisting moments (generated by the membrane forces $N_{xy,1}$ and $N_{xy,2}$), which are balanced directly by corresponding reaction couples. Without loss of generality, we

assume once again that $q_0 > 0$. As in ordinary Kirchhoff plate theory, the ‘‘Kirchhoff’’ twisting moment distribution along an edge is replaced by a statically equivalent system of vertical forces (distributed along that edge and concentrated at the corners) – Figure 3.6 illustrates this replacement for the edge $x = a$. The distributed vertical reactions on the edges $x = a$ and $y = b$ are thus found to be directed ‘‘upwards’’ (*i.e.*, opposite to the applied load) and to follow the sinusoidal laws

$$\begin{aligned} r(a, y) &= - \left(Q_x(a, y) + \frac{\partial M_{xy}^K}{\partial y}(a, y) \right) = - \left(\frac{\partial M_x^K}{\partial x}(a, y) + 2 \frac{\partial M_{xy}^K}{\partial y}(a, y) + Q_x^M(a, y) \right) = \\ &= \frac{\sum_{i=1}^2 E_i h_i^3}{12(1-\nu^2)} \left[\frac{\partial^3 W}{\partial x^3}(a, y) + (2-\nu) \frac{\partial^3 W}{\partial x \partial y^2}(a, y) \right] - G_{z,s} \frac{(z_2-z_1)^2}{h_s} \left(\frac{\partial W}{\partial x}(a, y) - \varphi_x(a, y) \right) = \\ &= \left\{ \frac{\sum_{i=1}^2 E_i h_i^3}{12(1-\nu^2)} \left[1 + \frac{a^2}{b^2} (2-\nu) \right] \frac{\pi^3}{a^3} W_0 + G_{z,s} \frac{(z_2-z_1)^2}{h_s} \left(\frac{\pi}{a} W_0 - X_0 \right) \right\} \sin \left(\frac{\pi y}{b} \right) \end{aligned} \quad (187)$$

$$\begin{aligned} r(x, b) &= - \left(Q_y(x, b) + \frac{\partial M_{xy}^K}{\partial x}(x, b) \right) = - \left(\frac{\partial M_y^K}{\partial y}(x, b) + 2 \frac{\partial M_{xy}^K}{\partial x}(x, b) + Q_y^M(x, b) \right) = \\ &= \frac{\sum_{i=1}^2 E_i h_i^3}{12(1-\nu^2)} \left[\frac{\partial^3 W}{\partial y^3}(x, b) + (2-\nu) \frac{\partial^3 W}{\partial x^2 \partial y}(x, b) \right] - G_{z,s} \frac{(z_2-z_1)^2}{h_s} \left(\frac{\partial W}{\partial y}(x, b) - \varphi_y(x, b) \right) = \\ &= \left\{ \frac{\sum_{i=1}^2 E_i h_i^3}{12(1-\nu^2)} \left[1 + \frac{b^2}{a^2} (2-\nu) \right] \frac{\pi^3}{b^3} W_0 + G_{z,s} \frac{(z_2-z_1)^2}{h_s} \left(\frac{\pi}{b} W_0 - Y_0 \right) \right\} \sin \left(\frac{\pi x}{a} \right). \end{aligned} \quad (188)$$

Clearly,

$$r(a, y) > |Q_x(a, y)|, \quad 0 < y < b \quad (189)$$

$$r(x, b) > |Q_y(x, b)|, \quad 0 < x < a. \quad (190)$$

From symmetry considerations, it may be concluded that equations (187) and (188) also represent the distribution of vertical support reactions along the edges $x = 0$ and $y = 0$, respectively. In addition, concentrated reactions in the ‘‘downward’’ direction (*i.e.*, in the direction of the applied load) occur at the four corners of the plate (Figure 3.7). These corner reactions are all equal, because of symmetry, and their magnitude is

$$R_0 = -2M_{xy}^K(a, b) = 2 \frac{\sum_{i=1}^2 E_i h_i^3}{12(1+\nu)} \frac{\partial^2 W}{\partial x \partial y}(a, b) = \frac{\sum_{i=1}^2 E_i h_i^3}{6(1+\nu)} \frac{\pi^2}{ab} W_0, \quad (191)$$

in which the factor 2 comes from the two perpendicular edges meeting at each corner. It is easily verified that

$$\int_0^a \int_0^b q_0 \sin\left(\frac{\pi x}{a}\right) \sin\left(\frac{\pi y}{b}\right) dy dx + 4R_0 - 2\left(\int_0^a r(x, b) dx + \int_0^b r(a, y) dy\right) =$$

$$= \frac{\sum_{i=1}^2 E_i h_i^3}{12(1-\nu^2)a} \left\{ \lambda - \pi^2(1+\rho^2)[\alpha + \pi^2(1+\rho^2)] \frac{W_0}{a} + \pi\alpha(X_0 + \rho Y_0) \right\} \frac{4}{\pi^2 \rho} = 0 \quad (192)$$

(cf. equation (173)), as required for equilibrium.

In the case of zero interaction between the two layers, which corresponds to $G_s = 0$ (and hence to $\alpha = 0$), one gets the deflection field

$$W = \frac{12(1-\nu^2)a^4 q_0}{\pi^4 \left(1 + \frac{a^2}{b^2}\right)^2 \sum_{i=1}^2 E_i h_i^3} \sin\left(\frac{\pi x}{a}\right) \sin\left(\frac{\pi y}{b}\right), \quad (193)$$

while the rotations φ_x and φ_y are identically zero. The plate behaves globally as a simply supported Kirchhoff plate with flexural rigidity $\frac{\sum_{i=1}^2 E_i h_i^3}{12(1-\nu^2)}$ (Timoshenko and Woinowsky-Krieger, 1959, § 27). The free interlayer slip is given by

$$\delta_x = -(z_2 - z_1) \frac{\partial W}{\partial x} = -(z_2 - z_1) \frac{12(1-\nu^2)a^3 q_0}{\pi^3 \left(1 + \frac{a^2}{b^2}\right)^2 \sum_{i=1}^2 E_i h_i^3} \cos\left(\frac{\pi x}{a}\right) \sin\left(\frac{\pi y}{b}\right) \quad (194)$$

$$\delta_y = -(z_2 - z_1) \frac{\partial W}{\partial y} = -(z_2 - z_1) \frac{12(1-\nu^2)a^4 q_0}{\pi^3 b \left(1 + \frac{a^2}{b^2}\right)^2 \sum_{i=1}^2 E_i h_i^3} \sin\left(\frac{\pi x}{a}\right) \cos\left(\frac{\pi y}{b}\right). \quad (195)$$

At the other end of the spectrum, when $G_{z,s} \rightarrow +\infty$ (that is, when $\alpha \rightarrow +\infty$) we find

$$\frac{W_0}{a} \rightarrow \frac{\lambda}{\pi^4 (1+\rho^2)^2 (1+\beta)} \quad (196)$$

$$X_0 \rightarrow \frac{\lambda}{\pi^3 (1+\rho^2)^2 (1+\beta)} \quad (197)$$

$$Y_0 \rightarrow \frac{\rho\lambda}{\pi^3 (1+\rho^2)^2 (1+\beta)}. \quad (198)$$

Therefore, for each $(x, y) \in [0, a] \times [0, b]$,

$$W(x, y) \rightarrow \frac{(1-\nu^2)a^4 q_0}{\pi^4 \left(1 + \frac{a^2}{b^2}\right)^2 \sum_{i=1}^2 E_i \left(\frac{h_i^3}{12} + z_i^2 h_i\right)} \sin\left(\frac{\pi x}{a}\right) \sin\left(\frac{\pi y}{b}\right) \quad (199)$$

$$\delta_x(x, y) \rightarrow 0 \quad (200)$$

$$\delta_y(x, y) \rightarrow 0. \quad (201)$$

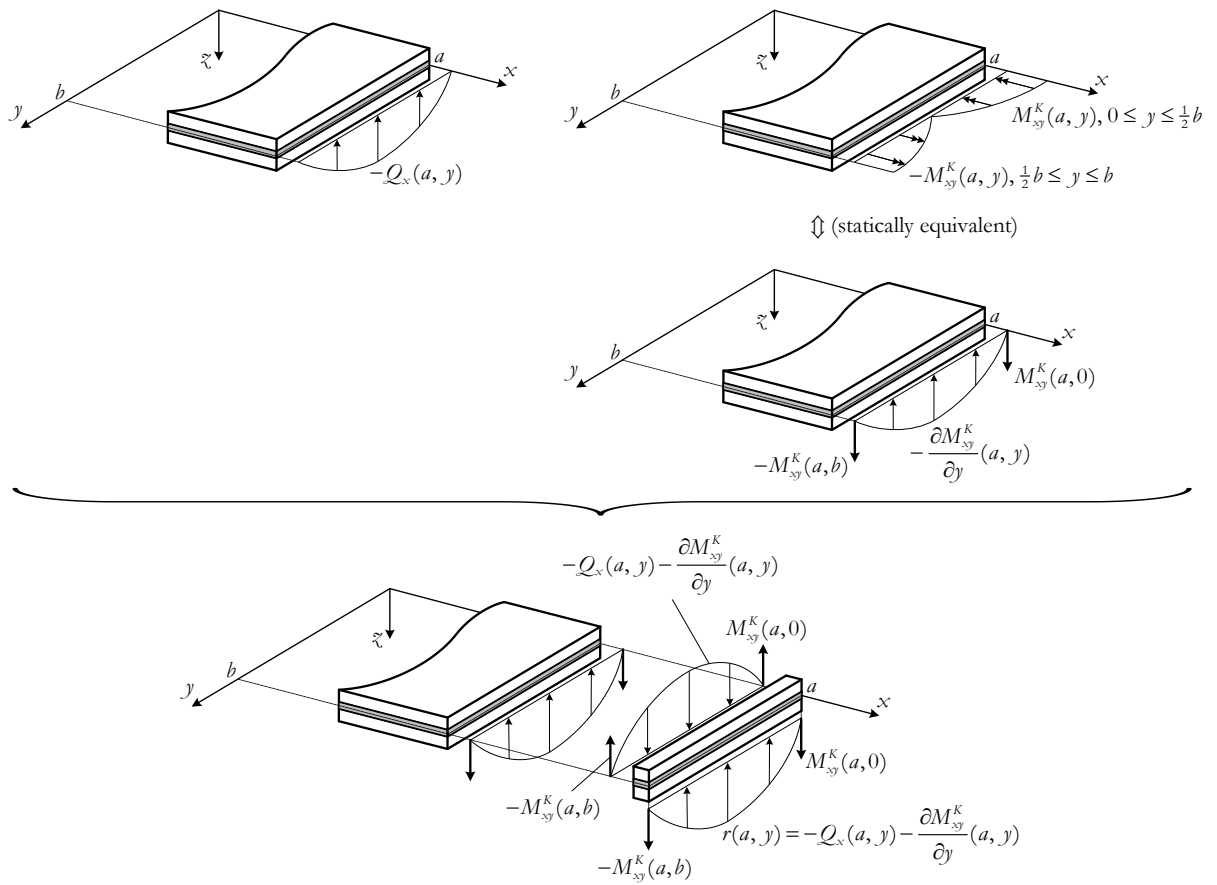


Figure 3.6: Illustrative example – Determination of the vertical support reactions

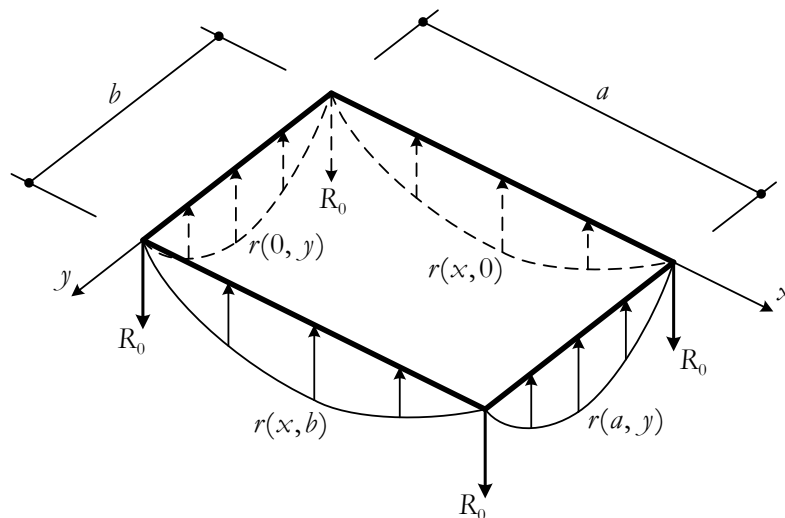


Figure 3.7: Illustrative problem – Vertical support reactions

In a pointwise sense, the behaviour of the plate tends to that of a simply supported Kirchhoff plate with flexural rigidity $\frac{1}{1-\nu^2} \sum_{i=1}^2 E_i \left(\frac{h_i^3}{12} + z_i^2 h_i \right) = (1 + \beta) \frac{\sum_{i=1}^2 E_i h_i^3}{12(1-\nu^2)}$ and no interlayer slip (full interaction).⁹

The results are therefore continuous across the whole range of zero, partial and full interaction.

Having solved a problem, one should not fail to look back at the completed solution, to re-examine the result and the path that led to it and to ask the question: “Can you use the result, or the method, for some other problem?” (Polya, 1973). Let us do just that. Suppose that the applied transverse load is given by

$$s_{z,1}^-(x, y) = q_{m \cdot n} \sin\left(\frac{m\pi x}{a}\right) \sin\left(\frac{n\pi y}{b}\right), \quad (202)$$

where m and n are positive integers. All other data remain the same. Then, proceeding as before, we find

$$W(x, y) = W_{m \cdot n} \sin\left(\frac{m\pi x}{a}\right) \sin\left(\frac{n\pi y}{b}\right) \quad (203)$$

$$\varphi_x(x, y) = X_{m \cdot n} \cos\left(\frac{m\pi x}{a}\right) \sin\left(\frac{n\pi y}{b}\right) \quad (204)$$

$$\varphi_y(x, y) = Y_{m \cdot n} \sin\left(\frac{m\pi x}{a}\right) \cos\left(\frac{n\pi y}{b}\right), \quad (205)$$

with

$$\frac{W_{m \cdot n}}{a} = \frac{\alpha + \pi^2 \beta (m^2 + n^2 \rho^2)}{\pi^4 (m^2 + n^2 \rho^2)^2 [\alpha(1 + \beta) + \pi^2 \beta (m^2 + n^2 \rho^2)]} \lambda_{m \cdot n} \quad (206)$$

$$X_{m \cdot n} = \frac{m\alpha}{\pi^3 (m^2 + n^2 \rho^2)^2 [\alpha(1 + \beta) + \pi^2 \beta (m^2 + n^2 \rho^2)]} \lambda_{m \cdot n} \quad (207)$$

⁹ In Foraboschi’s (2012) model, the slip components (2ξ and 2η in his notation) “approach zero without reaching zero” as $G_{z,s} \rightarrow +\infty$, a rather ambiguous statement that seems to mean that the pointwise limit for full interaction is actually not zero but some small quantity. This interpretation is in line with this author’s undue omission of the terms $-h_s \frac{\partial W}{\partial x}$ and $-h_s \frac{\partial W}{\partial y}$ in the definition of the slip components – see the remark after equations (54)-(55). It is also incorrect to assert that with zero slip “no shearing stress would be exchanged through the interfaces” – in the full interaction limit, the transverse shear stresses in the interlayer become reactive and no inconsistency arises.

$$Y_{m \cdot n} = \frac{n\alpha\rho}{\pi^3(m^2+n^2\rho^2)^2[\alpha(1+\beta)+\pi^2\beta(m^2+n^2\rho^2)]} \lambda_{m \cdot n} = \frac{n}{m}\rho X_{m \cdot n} \quad (208)$$

and

$$\lambda_{m \cdot n} = \frac{12(1-\nu^2)a^3 q_{m \cdot n}}{\sum_{i=1}^2 E_i h_i^3}. \quad (209)$$

It follows by linearity that if the load is given by a finite sum of the form

$$s_{z,1}^-(x, y) = \sum_{m=1}^M \sum_{n=1}^N q_{m \cdot n} \sin\left(\frac{m\pi x}{a}\right) \sin\left(\frac{n\pi y}{b}\right), \quad (210)$$

where M and N are positive integers, then

$$W(x, y) = \sum_{m=1}^M \sum_{n=1}^N W_{m \cdot n} \sin\left(\frac{m\pi x}{a}\right) \sin\left(\frac{n\pi y}{b}\right) \quad (211)$$

$$\varphi_x(x, y) = \sum_{m=1}^M \sum_{n=1}^N X_{m \cdot n} \cos\left(\frac{m\pi x}{a}\right) \sin\left(\frac{n\pi y}{b}\right) \quad (212)$$

$$\varphi_y(x, y) = \sum_{m=1}^M \sum_{n=1}^N Y_{m \cdot n} \sin\left(\frac{m\pi x}{a}\right) \cos\left(\frac{n\pi y}{b}\right). \quad (213)$$

As a concrete example, let us take

$$q_{m \cdot n} = \frac{4q_0}{ab} \int_0^a \int_0^b \sin\left(\frac{m\pi x}{a}\right) \sin\left(\frac{n\pi y}{b}\right) dy dx = \begin{cases} \frac{16q_0}{mn\pi^2} & \text{if } m \text{ and } n \text{ are odd} \\ 0 & \text{if } m \text{ or } n \text{ are even} \end{cases} \quad (214)$$

These are the Fourier coefficients of a uniform load q_0 on the interior of the rectangle $\bar{\Omega} = [0, a] \times [0, b]$ (e.g., Rektorys, 1994, pp. 688-689) – Figure 3.8. The maximum deflection occurs at the centre of the plate ($x = \frac{1}{2}a$, $y = \frac{1}{2}b$) and is given by

$$W_{max} = \sum_{m=1}^M \sum_{n=1}^N (-1)^{(m+n-2)/2} W_{m \cdot n}. \quad (215)$$

We considered the twelve case studies in Foraboschi (2012), all with $E_1 = E_2 = 70 \times 10^3 N/mm^2$ and $\nu_1 = \nu_2 = 0.22$. The remaining data and the calculated maximum deflections, accurate to five significant digits – to meet this target, it was necessary to consider between $M = N = 17$ and $M = N = 29$ in equation (215) – are presented in Table 3.1. The relative differences, Δ , between Foraboschi's results and ours vary from 0.35% to 18.20%. Though definite conclusions cannot be drawn on the basis of such a small and unsystematic data set, it appears that Δ increases with the shear modulus $G_{z,s}$ of the interlayer and with its thickness h_s . This would be consistent with Foraboschi's undue omission of the terms $-h_s \frac{\partial W}{\partial x}$ and $-h_s \frac{\partial W}{\partial y}$ in the

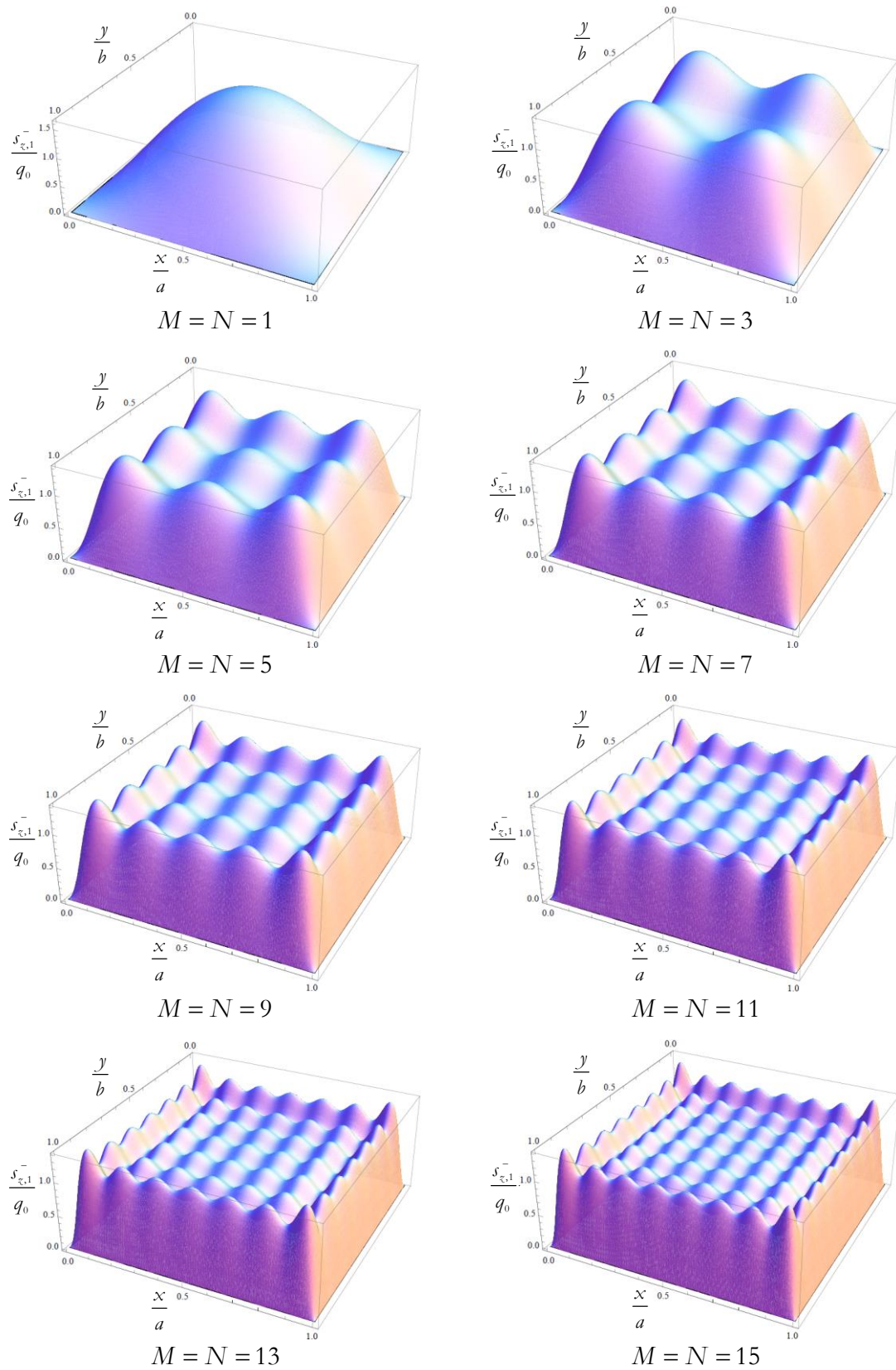


Figure 3.8: Truncated Fourier sine series expansion of a uniform load q_0 on the interior of the rectangle $[0, a] \times [0, b]$ – Gibbs phenomenon (e.g., Hewitt and Hewitt, 1979) is clearly visible

definition of the slip components δ_x and δ_y (and the consequential omission of the terms $\frac{\partial W}{\partial x}$ and $\frac{\partial W}{\partial y}$ in the definition of the interlayer transverse shear strains $\gamma_{xz, s}$ and $\gamma_{yz, s}$) – see the remark after equations (54)-(55). We also provide in Table 3.1 the maximum deflections corresponding to zero interaction ($\alpha = 0$) and to full interaction ($\alpha \rightarrow +\infty$), denoted respectively by W_{max}^0 and W_{max}^∞ . The non-dimensional ratio in the last column places the actual partial interaction situation in relation to these limits.

For the same twelve case studies, the maximum interlayer transverse shear strains

$$\gamma_{xz, s, max} = \frac{z_2 - z_1}{h_s} \sum_{m=1}^M \sum_{n=1}^N (-1)^{(n-1)/2} \left(m\pi \frac{W_{m,n}}{a} - X_{m,n} \right) \quad (216)$$

$$\gamma_{yz, s, max} = \frac{z_2 - z_1}{h_s} \sum_{m=1}^M \sum_{n=1}^N (-1)^{(m-1)/2} \left(n\pi\rho \frac{W_{m,n}}{a} - Y_{m,n} \right), \quad (217)$$

occurring at $(x, y) = (0, \frac{1}{2}b)$ and $(x, y) = (\frac{1}{2}a, 0)$, respectively, are shown in Table 3.2. Convergence is now significantly slower and, to obtain results that are accurate to four significant digits, it was necessary to consider up to $M = N = 45$. The relative differences Δ between Foraboschi's results and ours now range from -11.50% to 50.50% .

Table 3.1: Case studies – Maximum deflections

a	b	$h_1 = h_2$	h_s	$G_{z,s}$	q_0	W_{max} (mm)		Δ	W_{max}^0	W_{max}^∞	$\frac{W_{max}^0 - W_{max}^{present\ work}}{W_{max}^0 - W_{max}^\infty}$
						Present work	Foraboschi (2012)				
(mm)	(mm)	(mm)	(mm)	(N/mm ²)	(kN/m ²)			(%)	(mm)	(mm)	
1500	1000	4.0	1.52	0.85	2.0	8.7680	10.363	18.20	19.688	2.9327	0.652
2000	1500	5.0	1.14	0.44	1.20	12.549	13.909	10.80	26.277	4.7570	0.638
2000	1500	8.0	0.38	0.18	1.80	5.8544	5.9613	1.83	9.6231	2.2422	0.511
2000	2000	10.0	0.76	0.02	0.75	3.7846	3.7977	0.35	3.9762	0.88886	0.0621
2000	2000	10.0	0.76	1.50	0.75	1.3918	1.4593	4.85	3.9762	0.88886	0.837
3000	2000	10.0	0.76	0.04	0.75	6.6463	6.7039	0.87	7.5602	1.6901	0.156
3000	2000	10.0	0.76	3.00	0.75	2.0683	2.1807	5.43	7.5602	1.6901	0.936
6000	2000	10.0	0.76	0.07	0.75	9.1818	9.3404	1.73	11.973	2.6766	0.300
6000	2000	10.0	0.76	7.00	0.75	2.8809	3.0461	5.73	11.973	2.6766	0.978
4000	3000	12.0	1.52	0.60	1.50	16.202	17.330	6.96	38.017	7.9068	0.725
4000	3500	14.0	1.14	4.50	1.50	8.7250	9.2482	6.00	34.846	7.7291	0.963
4000	4000	18.0	0.38	1.20	1.50	6.1958	6.2896	1.51	21.817	5.2852	0.945

Table 3.2: Case studies – Maximum transverse shear strains in the interlayer

a	b	$h_1 = h_2$	h_s	$G_{z,s}$	q_0	$\gamma_{xz, s, max}$		Δ	$\gamma_{yz, s, max}$		Δ
						Present work	Foraboschi (2012)*		Present work	Foraboschi (2012)**	
(mm)	(mm)	(mm)	(mm)	(N/mm ²)	(kN/m ²)			(%)			(%)
1500	1000	4.0	1.52	0.85	2.0	0.06507	0.05758	-11.50	0.08379	0.07987	-4.68
2000	1500	5.0	1.14	0.44	1.20	0.09613	0.09082	-5.52	0.1158	0.1148	-0.87
2000	1500	8.0	0.38	0.18	1.80	0.1896	0.1930	1.79	0.2314	0.2452	5.95
2000	2000	10.0	0.76	0.02	0.75	0.08786	0.08518	-3.05	0.08786	0.08518	-3.05
2000	2000	10.0	0.76	1.50	0.75	0.01704	0.01847	8.41	0.01704	0.01847	8.41
3000	2000	10.0	0.76	0.04	0.75	0.1082	0.1044	-3.49	0.1471	0.1484	0.88
3000	2000	10.0	0.76	3.00	0.75	0.01053	0.01153	9.46	0.01269	0.01532	20.70
6000	2000	10.0	0.76	0.07	0.75	0.1054	0.1009	-4.30	0.1914	0.2324	21.40
6000	2000	10.0	0.76	7.00	0.75	0.005009	0.005105	1.92	0.006888	0.01037	50.50
4000	3000	12.0	1.52	0.60	1.50	0.08962	0.09034	0.81	0.1068	0.1134	6.16
4000	3500	14.0	1.14	4.50	1.50	0.01804	0.02058	14.10	0.01919	0.02260	17.80
4000	4000	18.0	0.38	1.20	1.50	0.05799	0.06742	16.30	0.05799	0.06742	16.30

* The results presented in this column follow from Table 1 (values of ξ_{m1}) and equation (11a) in Foraboschi (2012)

** The results presented in this column follow from Table 1 (values of η_{m1}) and equation (11b) in Foraboschi (2012)

4 SUMMARY AND CONCLUSIONS. RECOMMENDATIONS FOR FUTURE WORK

This dissertation presented a consistent derivation, from three-dimensional linear elasticity, of a two-dimensional mathematical model describing the bending and in-plane stretching behaviours, under a general system of quasi-static distributed loads and prescribed support displacements, of thin two-layer plates with partial shear interaction.

The dimensional reduction stage of the derivation is accomplished by means of Podio-Guidugli's method of internal constraints – the imposition of appropriate internal constraints, accompanied by reactive stresses, to plate-like bodies made of transversely isotropic materials, together with integration over the thickness. This is followed by a process of assembly or aggregation, in which the continuity of displacements and certain stress components across each layer/interlayer interface is enforced.

With this approach, a complete characterization of displacement, strain and stress fields that exactly satisfy the equations of three-dimensional linear elasticity was achieved. Moreover, one's choice of generalized variables brings to centre stage a number of illuminating similarities with the classical plate theories of Kirchhoff and Mindlin, thus providing valuable physical insight particularly when it comes to the specification of boundary conditions – a total of six boundary conditions are required, one more than in the theory of Mindlin and two more than in the theory of Kirchhoff – and the determination of support reactions.

Foraboschi's (2012) overlooks the fact that if the interlayer thickness is not negligible, then the slip cannot be defined merely as the relative displacement, parallel to the x, y -plane, between the end faces of the interlayer. This oversight carries over into the definition of the transverse shear strains and stresses in the interlayer, and so Foraboschi's model is flawed.

The closed-form solution to an illustrative example was proven to be continuous across the whole range of zero, partial and full interaction between the layers. A generalization of this illustrative example shows that the results (maximum deflections and maximum transverse shear strains in the interlayer) obtained with the proposed model can differ significantly from Foraboschi's predictions.

Possible applications include the analysis of laminated glass plates under quasi-static short-term loads in service conditions and within a limited temperature range. Additionally, this mathematical model can be improved and some recommendations for future research are as follows:

- To extend the range of applicability of the mathematical model derived in this dissertation by:
 - (i) addressing the dynamical response of layered plates, giving special consideration to impact loads);
 - (ii) incorporating geometrically non-linear effects, possibly using von Kármán plate theory;
 - (iii) adopting a viscoelastic and temperature-dependent material model for the interlayer.
- To develop finite element procedures for the numerical analysis of the mathematical model derived in this dissertation and its suggested extensions.
- To investigate the parameters that influence the most the mechanical behaviour of layered plates in general and laminated glass plates in particular.

APPENDIX 1: A SUMMARY, IN THE FORM OF A TONTI DIAGRAM, OF THE TOP-TIER FIELD EQUATIONS OF THE TWO- DIMENSIONAL MODEL

The objective of this appendix is twofold:

- (i) To offer an overall, sweeping view of the two-dimensional model developed in the body of the dissertation (of its top tier, to be precise);
- (ii) To underscore the basic ingredients – the building blocks, so to speak – and the dual structure of this model.

In the top-tier field equations, we can single out four sets of dependent variables (all of which are all real-valued functions defined on $\bar{\Omega} \subset \mathbb{R}^2$):

- (i) The generalized displacements and strains, collected in the column vectors

$$\mathbf{d} = \begin{Bmatrix} U \\ V \\ W \\ \varphi_x \\ \varphi_y \end{Bmatrix} \quad \boldsymbol{\varepsilon} = \begin{Bmatrix} \bar{\boldsymbol{\varepsilon}} \\ \boldsymbol{\chi}^K \\ \boldsymbol{\chi}^M \\ \boldsymbol{\gamma}^M \end{Bmatrix} = \begin{Bmatrix} \bar{\varepsilon}_x \\ \bar{\varepsilon}_y \\ \bar{\gamma}_{xy} \\ \chi_x^K \\ \chi_y^K \\ \chi_{xy}^K \\ \chi_x^M \\ \chi_y^M \\ \chi_{xy}^M \\ \gamma_{xz}^M \\ \gamma_{yz}^M \end{Bmatrix}, \quad (1.1)$$

which Tonti (2013, § 5.4.2) classifies as “configuration variables”;

- (ii) The plate loads (corresponding to the generalized displacements) and the active generalized stresses (conjugate to the generalized strains), arranged in the column vectors

$$\mathbf{q} = \left\{ \begin{array}{c} q_x \\ q_y \\ q_z + \frac{\partial m_x^K}{\partial x} + \frac{\partial m_y^K}{\partial y} \\ -m_x^M \\ -m_y^M \end{array} \right\} \quad \boldsymbol{\sigma}^{(a)} = \left\{ \begin{array}{c} \mathbf{N} \\ \mathbf{M}^K \\ \mathbf{M}^M \\ \mathbf{Q}^M \end{array} \right\} = \left\{ \begin{array}{c} N_x \\ N_y \\ N_{xy} \\ M_x^K \\ M_y^K \\ M_{xy}^K \\ M_x^M \\ M_y^M \\ M_{xy}^M \\ Q_x^M \\ Q_y^M \end{array} \right\}, \quad (1.2)$$

which Tonti (2013, § 5.4.1) classifies as “source variables”. It should be noted that the plate loads m_x^K and m_y^K are associated with derivatives of the generalized displacement W and not with independent generalized displacements in their own right. This is a direct consequence of the internal constraints A3.1.

The generalized displacements \mathbf{d} and the generalised strains $\boldsymbol{\varepsilon}$ are connected by the kinematic equation

$$\boldsymbol{\varepsilon} = \mathbf{Ld}, \quad (1.3)$$

where

$$\mathbf{L} = \begin{bmatrix} \mathbf{L}_1 & \mathbf{0} & \mathbf{0} \\ \mathbf{0} & \mathbf{L}_2 & \mathbf{0} \\ \mathbf{0} & \mathbf{0} & -\mathbf{L}_1 \\ \mathbf{0} & \mathbf{L}_3 & -\mathbf{I} \end{bmatrix} \quad (1.4)$$

is a formal linear differential operator¹⁰ with non-zero blocks

$$\mathbf{L}_1 = \begin{bmatrix} \frac{\partial}{\partial x} & 0 \\ 0 & \frac{\partial}{\partial y} \\ \frac{\partial}{\partial y} & \frac{\partial}{\partial x} \end{bmatrix} \quad \mathbf{L}_2 = - \begin{bmatrix} \frac{\partial^2}{\partial x^2} \\ \frac{\partial^2}{\partial y^2} \\ 2 \frac{\partial^2}{\partial x \partial y} \end{bmatrix} \quad \mathbf{L}_3 = \begin{bmatrix} \frac{\partial}{\partial x} \\ \frac{\partial}{\partial y} \end{bmatrix} \quad \mathbf{I} = \begin{bmatrix} 1 & 0 \\ 0 & 1 \end{bmatrix}. \quad (1.5)$$

Tonti (2013, § 6.6) calls (1.3), which agglutinates equations (45) to (48), a “definition equation”.

¹⁰ In this context, the word “formal” just means that the domain of the operator is not specified.

The active generalized stresses $\boldsymbol{\sigma}^{(a)}$ are related to the generalized strains $\boldsymbol{\varepsilon}$ through the constitutive relation

$$\boldsymbol{\sigma}^{(a)} = \mathbf{k}\boldsymbol{\varepsilon}, \quad (1.6)$$

where \mathbf{k} is the symmetric stiffness matrix

$$\mathbf{k} = \begin{bmatrix} \mathbf{k}_{11} & \mathbf{0} & \mathbf{k}_{13} & \mathbf{0} \\ \mathbf{0} & \mathbf{k}_{22} & \mathbf{0} & \mathbf{0} \\ \mathbf{k}_{13}^T = \mathbf{k}_{13} & \mathbf{0} & \mathbf{k}_{33} & \mathbf{0} \\ \mathbf{0} & \mathbf{0} & \mathbf{0} & \mathbf{k}_{44} \end{bmatrix} \quad (1.7)$$

with non-zero blocks

$$\mathbf{k}_{11} = \begin{bmatrix} \sum_{i=1}^2 \frac{E_i h_i}{1-\nu_i^2} & \sum_{i=1}^2 \frac{\nu_i E_i h_i}{1-\nu_i^2} & 0 \\ \sum_{i=1}^2 \frac{\nu_i E_i h_i}{1-\nu_i^2} & \sum_{i=1}^2 \frac{E_i h_i}{1-\nu_i^2} & 0 \\ 0 & 0 & \sum_{i=1}^2 \frac{E_i h_i}{2(1+\nu_i)} \end{bmatrix} \quad (1.8)$$

$$\mathbf{k}_{22} = \begin{bmatrix} \sum_{i=1}^2 \frac{E_i h_i^3}{12(1-\nu_i^2)} & \sum_{i=1}^2 \frac{\nu_i E_i h_i^3}{12(1-\nu_i^2)} & 0 \\ \sum_{i=1}^2 \frac{\nu_i E_i h_i^3}{12(1-\nu_i^2)} & \sum_{i=1}^2 \frac{E_i h_i^3}{12(1-\nu_i^2)} & 0 \\ 0 & 0 & \sum_{i=1}^2 \frac{E_i h_i^3}{24(1+\nu_i)} \end{bmatrix} \quad (1.9)$$

$$\mathbf{k}_{33} = \begin{bmatrix} \sum_{i=1}^2 \frac{z_i^2 E_i h_i}{1-\nu_i^2} & \sum_{i=1}^2 \frac{z_i^2 \nu_i E_i h_i}{1-\nu_i^2} & 0 \\ \sum_{i=1}^2 \frac{z_i^2 \nu_i E_i h_i}{1-\nu_i^2} & \sum_{i=1}^2 \frac{z_i^2 E_i h_i}{1-\nu_i^2} & 0 \\ 0 & 0 & \sum_{i=1}^2 \frac{z_i^2 E_i h_i}{2(1+\nu_i)} \end{bmatrix} \quad (1.10)$$

$$\mathbf{k}_{13} = \begin{bmatrix} \sum_{i=1}^2 \frac{z_i E_i h_i}{1-\nu_i^2} & \sum_{i=1}^2 \frac{z_i \nu_i E_i h_i}{1-\nu_i^2} & 0 \\ \sum_{i=1}^2 \frac{z_i \nu_i E_i h_i}{1-\nu_i^2} & \sum_{i=1}^2 \frac{z_i E_i h_i}{1-\nu_i^2} & 0 \\ 0 & 0 & \sum_{i=1}^2 \frac{z_i E_i h_i}{2(1+\nu_i)} \end{bmatrix} \quad (1.11)$$

$$\mathbf{k}_{44} = G_{z,s} \frac{(z_2 - z_1)^2}{h_s} \mathbf{I} \quad (1.12)$$

(cf. equations (70)-(79)). Observe that

$$\mathbf{k}_{11} = \sum_{i=1}^2 \mathbf{k}_{m,i} \quad \mathbf{k}_{22} = \sum_{i=1}^2 \mathbf{k}_{b,i} \quad \mathbf{k}_{33} = \sum_{i=1}^2 z_i^2 \mathbf{k}_{m,i} \quad \mathbf{k}_{13} = \sum_{i=1}^2 z_i \mathbf{k}_{m,i}, \quad (1.13)$$

where

$$\mathbf{k}_{m,i} = \frac{E_i h_i}{1-\nu_i^2} \begin{bmatrix} 1 & \nu_i & 0 \\ \nu_i & 1 & 0 \\ 0 & 0 & \frac{1-\nu_i}{2} \end{bmatrix} \quad (1.14)$$

$$\mathbf{k}_{b,i} = \frac{E_i h_i^3}{12(1-\nu_i^2)} \begin{bmatrix} 1 & \nu_i & 0 \\ \nu_i & 1 & 0 \\ 0 & 0 & \frac{1-\nu_i}{2} \end{bmatrix} \quad (1.15)$$

are the membrane and bending stiffness matrices of each individual layer i ($i = 1,2$) – *e.g.*, Blaauwendraad (2010, pp. 13 and 63).

The plate loads \mathbf{q} are related to the active generalized stresses $\boldsymbol{\sigma}^{(a)}$ via the equilibrium condition

$$\mathbf{L}^\dagger \boldsymbol{\sigma}^{(a)} = \mathbf{q}, \quad (1.16)$$

where (the superscript “T” means transposition)

$$\mathbf{L}^\dagger = \begin{bmatrix} -\mathbf{L}_1^T & \mathbf{0} & \mathbf{0} & \mathbf{0} \\ \mathbf{0} & \mathbf{L}_2^T & \mathbf{0} & -\mathbf{L}_3^T \\ \mathbf{0} & \mathbf{0} & \mathbf{L}_1^T & -\mathbf{I} \end{bmatrix} \quad (1.17)$$

is the formal adjoint of \mathbf{L} (*e.g.*, Lanczos, 1996, §§ 4.10-4.12).¹¹ The duality between kinematics and statics (*e.g.*, Carpinteri, 1997, § 8.3) is explicit.

The three equations (1.3), (1.6) and (1.16) can be combined to yield, in Tonti’s terminology (TONTI 2013, § 6.1), the “fundamental equation”

$$\mathbf{L}^\dagger \mathbf{k} \mathbf{L} \mathbf{d} = \mathbf{q}. \quad (1.18)$$

This is just a compact matrix format for the set of equations (140) to (144). The process is summarised in Figure A1.1 by means of a Tonti diagram (Tonti, 1972).

¹¹ This means that

$$\iint_{\Omega} \boldsymbol{\sigma}^{(a)T} \mathbf{L} \mathbf{d} \, dx dy - \iint_{\Omega} \mathbf{d}^T \mathbf{L}^\dagger \boldsymbol{\sigma}^{(a)} \, dx dy = \text{boundary term}$$

for any given column vectors \mathbf{d} and $\boldsymbol{\sigma}^{(a)}$, unrelated to each other (*i.e.*, it is not required that $\boldsymbol{\sigma}^{(a)} = \mathbf{k} \mathbf{L} \mathbf{d}$) and whose elements are sufficiently differentiable but are not subject to specific boundary conditions.

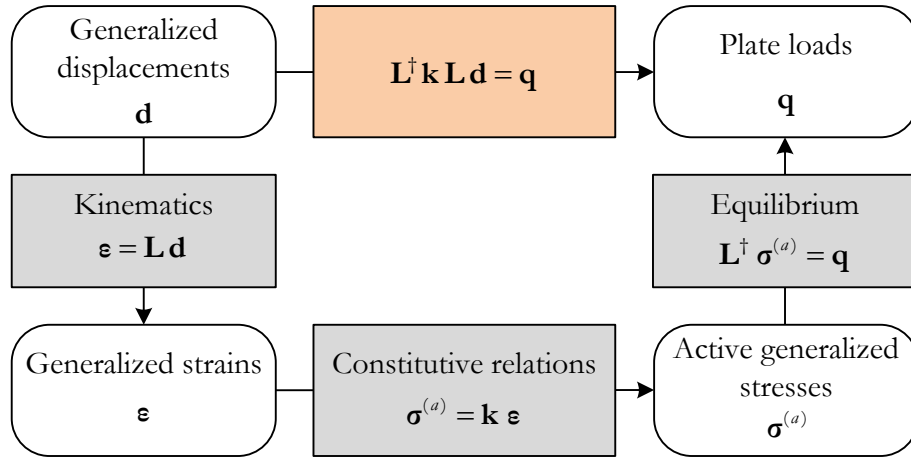


Figure A1.1: Tonti diagram of structural relations

To the four sets of dependent variables already described, we can now add the reactive generalized stresses, collected in the column vector

$$\boldsymbol{\sigma}^{(r)} = \begin{Bmatrix} Q_x^{(r)} \\ Q_y^{(r)} \end{Bmatrix}. \quad (1.19)$$

These reactive generalized stresses satisfy the equilibrium condition

$$\boldsymbol{\sigma}^{(r)} = \mathbf{L}_1^T \mathbf{M}^K + \begin{Bmatrix} m_x^K \\ m_y^K \end{Bmatrix}, \quad (1.20)$$

which can be further developed into

$$\boldsymbol{\sigma}^{(r)} = \mathbf{L}_1^T \mathbf{k}_{22} \mathbf{L}_2 W + \begin{Bmatrix} m_x^K \\ m_y^K \end{Bmatrix}. \quad (1.21)$$

APPENDIX 2: THE REACTIVE STRESS FIELDS $\tau_{xz,i}$, $\tau_{yz,i}$ AND $\sigma_{z,i}$ ON EACH LAYER; THE REACTIVE STRESS FIELD $\sigma_{z,s}$ ON THE INTERLAYER

This appendix provides an explicit characterization of the reactive stress fields in terms of upper-tier generalized displacements and in terms of intermediate-tier generalized stresses.

The transverse shear stress field $\tau_{xz,1}$ on the “top” layer ($i = 1$) must satisfy the Cauchy equation (84) and the traction boundary condition (87₁). These relations, when combined with the bottom-tier constitutive equations (56) and (58) and with the kinematic equations (40)-(42), yield

$$\begin{aligned} \tau_{xz,1}(x, y, z) &= \tau_{xz,1}(x, y, z_1 - \frac{1}{2}h_1) - \int_{z_1 - \frac{1}{2}h_1}^z \left(\frac{\partial \sigma_{x,1}}{\partial x}(x, y, \zeta) + \frac{\partial \tau_{xy,1}}{\partial y}(x, y, \zeta) + b_{x,1}(x, y, \zeta) \right) d\zeta = \\ &= -s_{x,1}^- - \frac{E_1}{1-\nu_1^2} \left\{ \left[z - \left(z_1 - \frac{h_1}{2} \right) \right] \left[\frac{\partial^2 U}{\partial x^2} + \frac{1-\nu_1}{2} \frac{\partial^2 U}{\partial y^2} + \frac{1+\nu_1}{2} \frac{\partial^2 V}{\partial x \partial y} - \right. \right. \\ &\quad \left. \left. - z_1 \left(\frac{\partial^2 \varphi_x}{\partial x^2} + \frac{1-\nu_1}{2} \frac{\partial^2 \varphi_x}{\partial y^2} + \frac{1+\nu_1}{2} \frac{\partial^2 \varphi_y}{\partial x \partial y} \right) \right] - \right. \\ &\quad \left. - \frac{1}{2} \left[(z - z_1)^2 - \left(\frac{h_1}{2} \right)^2 \right] \frac{\partial}{\partial x} \nabla^2 W \right\} - \int_{z_1 - \frac{1}{2}h_1}^z b_{x,1}(x, y, \zeta) d\zeta, \quad (2.1) \end{aligned}$$

with $z_1 - \frac{1}{2}h_1 \leq z \leq z_1 + \frac{1}{2}h_1$. The intermediate-tier constitutive equations (60), (62), (63) and (65) enable us to write this result in the following alternative form:

$$\begin{aligned} \tau_{xz,1}(x, y, z) &= -s_{x,1}^- - \frac{1}{h_1} \left[z - \left(z_1 - \frac{h_1}{2} \right) \right] \left(\frac{\partial N_{x,1}}{\partial x} + \frac{\partial N_{xy,1}}{\partial y} \right) - \\ &\quad - \frac{6}{h_1^3} \left[(z - z_1)^2 - \left(\frac{h_1}{2} \right)^2 \right] \left(\frac{\partial M_{x,1}}{\partial x} + \frac{\partial M_{xy,1}}{\partial y} \right) - \int_{z_1 - \frac{1}{2}h_1}^z b_{x,1}(x, y, \zeta) d\zeta. \quad (2.2) \end{aligned}$$

The unused traction boundary condition (87₂) is automatically satisfied. Indeed, in view of (97) and (100), we find

$$\begin{aligned}
\tau_{xz,1}(x, y, z_1 + \frac{1}{2}h_1) &= -s_{x,1}^- - \left(\frac{\partial N_{x,1}}{\partial x} + \frac{\partial N_{xy,1}}{\partial y} \right) - \int_{z_1 - \frac{1}{2}h_1}^{z_1 + \frac{1}{2}h_1} b_{x,1} dz = \\
&= -s_{x,1}^- + q_{x,1} - \int_{z_1 - \frac{1}{2}h_1}^{z_1 + \frac{1}{2}h_1} b_{x,1} dz = s_{x,1}^+.
\end{aligned} \tag{2.3}$$

Moreover, observe that (cf. equation (103))

$$\begin{aligned}
\int_{z_1 - \frac{1}{2}h_1}^{z_1 + \frac{1}{2}h_1} \tau_{xz,1} dz &= -h_1 s_{x,1}^- - \frac{h_1}{2} \left(\frac{\partial N_{x,1}}{\partial x} + \frac{\partial N_{xy,1}}{\partial y} \right) + \frac{\partial M_{x,1}}{\partial x} + \frac{\partial M_{xy,1}}{\partial y} - \\
&\quad - \int_{z_1 - \frac{1}{2}h_1}^{z_1 + \frac{1}{2}h_1} \left(\int_{z_1 - \frac{1}{2}h_1}^z b_{x,1}(x, y, \zeta) d\zeta \right) dz = \\
&= h_1 \left(\frac{1}{2} q_{x,1} - s_{x,1}^- \right) + \frac{\partial M_{x,1}}{\partial x} + \frac{\partial M_{xy,1}}{\partial y} - \frac{h_1}{2} \int_{z_1 - \frac{1}{2}h_1}^{z_1 + \frac{1}{2}h_1} b_{x,1} dz + \\
&\quad + \int_{z_1 - \frac{1}{2}h_1}^{z_1 + \frac{1}{2}h_1} (z - z_1) b_{x,1} dz = \\
&= \frac{\partial M_{x,1}}{\partial x} + \frac{\partial M_{xy,1}}{\partial y} + m_{x,1} = Q_{x,1}.
\end{aligned} \tag{2.4}$$

We can apply a similar line of reasoning to obtain the transverse shear stress field $\tau_{xz,2}$ on the “bottom” layer ($i = 2$). The only difference worthy of mention is that we now use the traction boundary condition (87₂), instead of (87₁).¹² The end result is

$$\begin{aligned}
\tau_{xz,2}(x, y, z) &= \tau_{xz,1}(x, y, z_2 + \frac{1}{2}h_2) + \int_z^{z_2 + \frac{1}{2}h_2} \left(\frac{\partial \sigma_{x,2}}{\partial x}(x, y, \zeta) + \frac{\partial \tau_{xy,2}}{\partial y}(x, y, \zeta) + b_{x,2}(x, y, \zeta) \right) d\zeta = \\
&= s_{x,2}^+ + \frac{E_2}{1-\nu_2^2} \left\{ \left(z_2 + \frac{h_2}{2} - z \right) \left[\frac{\partial^2 U}{\partial x^2} + \frac{1-\nu_2}{2} \frac{\partial^2 U}{\partial y^2} + \frac{1+\nu_2}{2} \frac{\partial^2 V}{\partial x \partial y} - \right. \right. \\
&\quad \left. \left. - z_2 \left(\frac{\partial^2 \varphi_x}{\partial x^2} + \frac{1-\nu_2}{2} \frac{\partial^2 \varphi_x}{\partial y^2} + \frac{1+\nu_2}{2} \frac{\partial^2 \varphi_y}{\partial x \partial y} \right) \right] - \right. \\
&\quad \left. - \frac{1}{2} \left[\left(\frac{h_2}{2} \right)^2 - (z - z_2)^2 \right] \frac{\partial}{\partial x} \nabla^2 W \right\} + \int_z^{z_2 + \frac{1}{2}h_2} b_{x,2}(x, y, \zeta) d\zeta =
\end{aligned}$$

¹² With regard to the composite plate as a whole, $s_{x,1}^-$ and $s_{x,2}^+$ are given loads (part of the data), while $s_{x,1}^+$ and $s_{x,2}^-$ are internal forces and, as such, derived quantities:

$$s_{x,1}^+ = -s_{x,2}^- = G_{z,s} \frac{z_2 - z_1}{h_s} \left(\frac{\partial W}{\partial x} - \varphi_x \right).$$

$$\begin{aligned}
&= s_{x,2}^+ + \frac{1}{h_2} \left(z_2 + \frac{h_2}{2} - z \right) \left(\frac{\partial N_{x,2}}{\partial x} + \frac{\partial N_{xy,2}}{\partial y} \right) + \\
&\quad + \frac{6}{h_2^3} \left[\left(\frac{h_2}{2} \right)^2 - (z - z_2)^2 \right] \left(\frac{\partial M_{x,2}}{\partial x} + \frac{\partial M_{xy,2}}{\partial y} \right) + \int_z^{z_2 + \frac{1}{2}h_2} b_{x,2}(x, y, \zeta) d\zeta, \quad (2.5)
\end{aligned}$$

with $z_2 - \frac{1}{2}h_2 \leq z \leq z_2 + \frac{1}{2}h_2$, and once again we have

$$\begin{aligned}
\tau_{xz,2}(x, y, z_2 - \frac{1}{2}h_2) &= s_{x,2}^+ + \frac{\partial N_{x,2}}{\partial x} + \frac{\partial N_{xy,2}}{\partial y} + \int_{z_2 - \frac{1}{2}h_2}^{z_2 + \frac{1}{2}h_2} b_{x,2} dz = \\
&= s_{x,2}^+ - q_{x,2} + \int_{z_2 - \frac{1}{2}h_2}^{z_2 + \frac{1}{2}h_2} b_{x,2} dz = -s_{x,2}^- \quad (2.6)
\end{aligned}$$

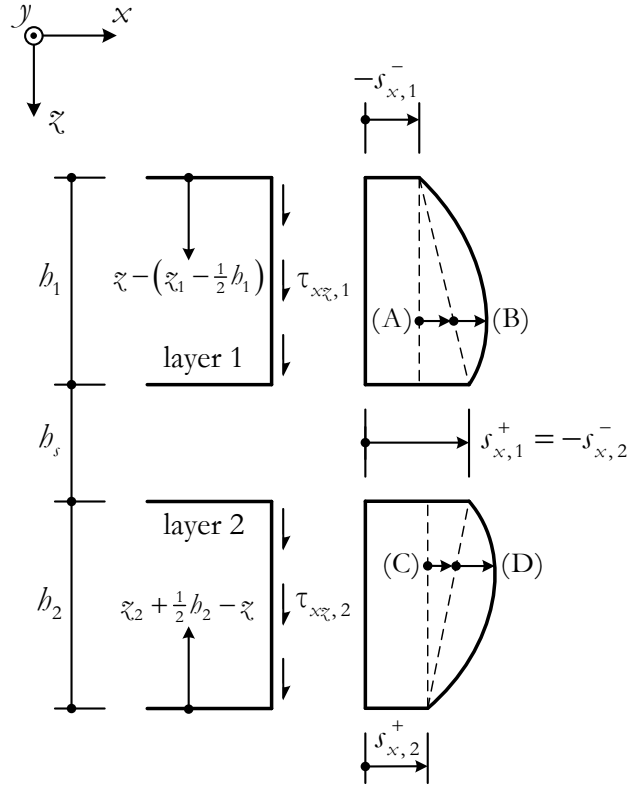
$$\begin{aligned}
\int_{z_2 - \frac{1}{2}h_2}^{z_2 + \frac{1}{2}h_2} \tau_{xz,2} dz &= h_2 s_{x,2}^+ + \frac{h_2}{2} \left(\frac{\partial N_{x,2}}{\partial x} + \frac{\partial N_{xy,2}}{\partial y} \right) + \frac{\partial M_{x,2}}{\partial x} + \frac{\partial M_{xy,2}}{\partial y} + \\
&\quad + \int_{z_2 - \frac{1}{2}h_2}^{z_2 + \frac{1}{2}h_2} \left(\int_z^{z_2 + \frac{1}{2}h_2} b_{x,2}(x, y, \zeta) d\zeta \right) dz = \\
&= h_2 \left(s_{x,2}^+ - \frac{1}{2} q_{x,2} \right) + \frac{\partial M_{x,2}}{\partial x} + \frac{\partial M_{xy,2}}{\partial y} + \frac{h_2}{2} \int_{z_2 - \frac{1}{2}h_2}^{z_2 + \frac{1}{2}h_2} b_{x,2} dz + \\
&\quad + \int_{z_2 - \frac{1}{2}h_2}^{z_2 + \frac{1}{2}h_2} (z - z_2) b_{x,2} dz = \\
&= \frac{\partial M_{x,2}}{\partial x} + \frac{\partial M_{xy,2}}{\partial y} + m_{x,2} = Q_{x,2}. \quad (2.7)
\end{aligned}$$

Figure A2.1 shows a schematic representation of the through-the-thickness distribution of shear stresses $\tau_{xz,i}$ for the special case in which the body forces $b_{x,i}$ are independent of z .

Analogous results concerning the fields $\tau_{yz,1}$ and $\tau_{yz,2}$ are obtained by the simple expedient of systematically interchanging x with y and U with V .

Now that the stress fields $\tau_{xz,i}$ and $\tau_{yz,i}$ are known in both layers, we can integrate equation (86) with respect to z , subject to (89₁) if $i = 1$ or (89₂) if $i = 2$, to obtain

$$\sigma_{z,1}(x, y, z) = \sigma_{z,1} \left(x, y, z_1 - \frac{1}{2}h_1 \right) - \int_{z_1 - \frac{1}{2}h_1}^z \left(\frac{\partial \tau_{xz,1}}{\partial x}(x, y, \zeta) + \frac{\partial \tau_{yz,1}}{\partial y}(x, y, \zeta) + b_{z,1}(x, y, \zeta) \right) d\zeta =$$



$$\begin{aligned}
 (A) &= - \left[z - \left(z_1 - \frac{h_1}{2} \right) \right] \left[\frac{1}{h_1} \left(\frac{\partial N_{x,1}}{\partial x} + \frac{\partial N_{xy,1}}{\partial y} \right) + b_{x,1} \right] \\
 (B) &= - \frac{6}{h_1^3} \left[z - \left(z_1 - \frac{h_1}{2} \right) \right] \left[z - \left(z_1 - \frac{h_1}{2} \right) - h_1 \right] \left(\frac{\partial M_{x,1}}{\partial x} + \frac{\partial M_{xy,1}}{\partial y} \right) \\
 (C) &= \left(z_2 + \frac{h_2}{2} - z \right) \left[\frac{1}{h_2} \left(\frac{\partial N_{x,2}}{\partial x} + \frac{\partial N_{xy,2}}{\partial y} \right) + b_{x,2} \right] \\
 (D) &= - \frac{6}{h_2^3} \left(z_2 + \frac{h_2}{2} - z \right) \left(z_2 + \frac{h_2}{2} - z - h_2 \right) \left(\frac{\partial M_{x,2}}{\partial x} + \frac{\partial M_{xy,2}}{\partial y} \right)
 \end{aligned}$$

Figure A2.1: Through-the-thickness distribution of shear stresses $\tau_{xz,i}$ ($i = 1, 2$), assuming that the body forces $b_{x,i}$ are independent of z

$$\begin{aligned}
 &= -s_{z,1}^- - \int_{z_1 - \frac{1}{2}h_1}^z b_{z,1}(x, y, \zeta) d\zeta + \left[z - \left(z_1 - \frac{h_1}{2} \right) \right] \left(\frac{\partial s_{x,1}^-}{\partial x} + \frac{\partial s_{y,1}^-}{\partial y} \right) + \\
 &+ \int_{z_1 - \frac{1}{2}h_1}^z \left[\int_{z_1 - \frac{1}{2}h_1}^{\zeta} \left(\frac{\partial}{\partial x} b_{x,1}(x, y, \psi) + \frac{\partial}{\partial y} b_{y,1}(x, y, \psi) \right) d\psi \right] d\zeta + \\
 &+ \frac{E_1}{2(1-\nu_1^2)} \left[z - \left(z_1 - \frac{h_1}{2} \right) \right]^2 \left[\frac{\partial}{\partial x} \nabla^2 U + \frac{\partial}{\partial y} \nabla^2 V - z_1 \left(\frac{\partial}{\partial x} \nabla^2 \varphi_x + \frac{\partial}{\partial y} \nabla^2 \varphi_y \right) \right] - \\
 &- \frac{E_1}{6(1-\nu_1^2)} \left[z - \left(z_1 - \frac{h_1}{2} \right) \right]^2 (z - z_1 - h_1) \nabla^4 W =
 \end{aligned}$$

$$\begin{aligned}
&= -s_{z,1}^- - \int_{z_1 - \frac{1}{2}h_1}^z b_{z,1}(x, y, \zeta) d\zeta + \left[z - \left(z_1 - \frac{h_1}{2} \right) \right] \left(\frac{\partial s_{x,1}^-}{\partial x} + \frac{\partial s_{y,1}^-}{\partial y} \right) + \\
&\quad + \int_{z_1 - \frac{1}{2}h_1}^z \left[\int_{z_1 - \frac{1}{2}h_1}^{\zeta} \left(\frac{\partial}{\partial x} b_{x,1}(x, y, \psi) + \frac{\partial}{\partial y} b_{y,1}(x, y, \psi) \right) d\psi \right] d\zeta + \\
&\quad + \frac{1}{2h_1} \left[z - \left(z_1 - \frac{h_1}{2} \right) \right]^2 \left(\frac{\partial^2 N_{x,1}}{\partial x^2} + 2 \frac{\partial^2 N_{xy,1}}{\partial x \partial y} + \frac{\partial^2 N_{y,1}}{\partial y^2} \right) + \\
&\quad + \frac{2}{h_1^3} \left[z - \left(z_1 - \frac{h_1}{2} \right) \right]^2 (z - z_1 - h_1) \left(\frac{\partial^2 M_{x,1}}{\partial x^2} + 2 \frac{\partial^2 M_{xy,1}}{\partial x \partial y} + \frac{\partial^2 M_{y,1}}{\partial y^2} \right), \tag{2.8}
\end{aligned}$$

with $z_1 - \frac{1}{2}h_1 \leq z \leq z_1 + \frac{1}{2}h_1$, and

$$\begin{aligned}
\sigma_{z,2}(x, y, z) &= \sigma_{z,2} \left(x, y, z_2 + \frac{1}{2}h_2 \right) + \int_z^{z_2 + \frac{1}{2}h_2} \left(\frac{\partial \tau_{xz,2}}{\partial x}(x, y, \zeta) + \frac{\partial \tau_{yz,2}}{\partial y}(x, y, \zeta) + b_{z,2}(x, y, \zeta) \right) d\zeta = \\
&= s_{z,2}^+ + \int_z^{z_2 + \frac{1}{2}h_2} b_{z,2}(x, y, \zeta) d\zeta + \left(z_2 + \frac{h_2}{2} - z \right) \left(\frac{\partial s_{x,2}^+}{\partial x} + \frac{\partial s_{y,2}^+}{\partial y} \right) + \\
&\quad + \int_z^{z_2 + \frac{1}{2}h_2} \left[\int_{\zeta}^{z_2 + \frac{1}{2}h_2} \left(\frac{\partial}{\partial x} b_{x,2}(x, y, \psi) + \frac{\partial}{\partial y} b_{y,2}(x, y, \psi) \right) d\psi \right] d\zeta + \\
&\quad + \frac{E_2}{2(1-\nu_2^2)} \left(z_2 + \frac{h_2}{2} - z \right)^2 \left[\frac{\partial}{\partial x} \nabla^2 U + \frac{\partial}{\partial y} \nabla^2 V - z_2 \left(\frac{\partial}{\partial x} \nabla^2 \varphi_x + \frac{\partial}{\partial y} \nabla^2 \varphi_y \right) \right] + \\
&\quad + \frac{E_2}{6(1-\nu_2^2)} \left(z_2 + \frac{h_2}{2} - z \right)^2 (z_2 - h_2 - z) \nabla^4 W = \\
&= s_{z,2}^+ + \int_z^{z_2 + \frac{1}{2}h_2} b_{z,2}(x, y, \zeta) d\zeta + \left(z_2 + \frac{h_2}{2} - z \right) \left(\frac{\partial s_{x,2}^+}{\partial x} + \frac{\partial s_{y,2}^+}{\partial y} \right) + \\
&\quad + \int_z^{z_2 + \frac{1}{2}h_2} \left[\int_{\zeta}^{z_2 + \frac{1}{2}h_2} \left(\frac{\partial}{\partial x} b_{x,2}(x, y, \psi) + \frac{\partial}{\partial y} b_{y,2}(x, y, \psi) \right) d\psi \right] d\zeta + \\
&\quad + \frac{1}{2h_2} \left(z_2 + \frac{h_2}{2} - z \right)^2 \left(\frac{\partial^2 N_{x,2}}{\partial x^2} + 2 \frac{\partial^2 N_{xy,2}}{\partial x \partial y} + \frac{\partial^2 N_{y,2}}{\partial y^2} \right) - \\
&\quad - \frac{2}{h_2^3} \left(z_2 + \frac{h_2}{2} - z \right)^2 (z_2 - h_2 - z) \left(\frac{\partial^2 M_{x,2}}{\partial x^2} + 2 \frac{\partial^2 M_{xy,2}}{\partial x \partial y} + \frac{\partial^2 M_{y,2}}{\partial y^2} \right), \tag{2.9}
\end{aligned}$$

with $z_2 - \frac{1}{2}h_2 \leq z \leq z_2 + \frac{1}{2}h_2$. The reader may easily verify that

$$\sigma_{z,1} \left(x, y, z_1 + \frac{1}{2}h_1 \right) = s_{z,1}^+ \quad \sigma_{z,2} \left(x, y, z_2 - \frac{1}{2}h_2 \right) = -s_{z,2}^-. \tag{2.10}$$

Having calculated $s_{z,1}^+$, we can set $\sigma_{z,s}(x, y, z_s - \frac{1}{2}h_s) = -s_{z,s}^- = s_{z,1}^+$ and then the reactive stress field $\sigma_{z,s}$ on the interlayer is given by

$$\begin{aligned}\sigma_{z,s}(x, y, z) &= \sigma_{z,s}(x, y, z_s - \frac{1}{2}h_s) - \int_{z_s - \frac{1}{2}h_s}^z \left(\frac{\partial \tau_{xz,s}}{\partial x}(x, y, \zeta) + \frac{\partial \tau_{yz,s}}{\partial y}(x, y, \zeta) \right) d\zeta = \\ &= s_{z,1}^+ - G_{z,s} \frac{z_2 - z_1}{h_s} \left[z - \left(z_s - \frac{h_s}{2} \right) \right] \left(\nabla^2 W - \frac{\partial \varphi_x}{\partial x} - \frac{\partial \varphi_y}{\partial y} \right) = \\ &= s_{z,1}^+ - \frac{1}{h_s} \left[z - \left(z_s - \frac{h_s}{2} \right) \right] \left(\frac{\partial Q_{x,s}}{\partial x} + \frac{\partial Q_{y,s}}{\partial y} \right),\end{aligned}\quad (2.11)$$

with $z_s - \frac{1}{2}h_s \leq z \leq z_s + \frac{1}{2}h_s$. Clearly,

$$\sigma_{z,s}(x, y, z_s + \frac{1}{2}h_s) = s_{z,s}^+ = -s_{z,2}^-.\quad (2.12)$$

REFERENCES

- Andrade, A. (2013). “One-Dimensional Models for the Spatial Behaviour of Tapered Thin-Walled Bars with Open Cross-Sections: Static, Dynamic and Buckling Analyses”. PhD Thesis, University of Coimbra.
- Andrade, A., Providência, P., Cabrera, F. (2019). “Vibration of Composite Beams with Deformable Shear Connection: Mathematical Modelling and Numerical Solution Using General-Purpose Software for Two-Point Boundary Value Problems”. *Journal of Sound and Vibration*, Vol. 463, Article 114913.
- Babuska, I., Oden, J.T. (2004). “Verification and Validation in Computational Engineering and Science: Basic Concepts”. *Computer Methods in Applied Mechanics and Engineering*, Vol. 193, Issues 36-38, pp. 4057-4066.
- Bartle, R.G. (1976). “The Elements of Real Analysis” (2nd edition). Wiley, New York.
- Blaauwendraad, J. (2010). “Plates and FEM – Surprises and Pitfalls”. Springer, Dordrecht.
- Carpinteri, A. (1997). “Structural Mechanics – A Unified Approach”. Taylor & Francis, London.
- Dias da Silva, V. (2006). “Mechanics and Strength of Materials”. Springer, Berlin.
- Ferreira, M., Andrade, A., Providência, P., Cabrera, F. (2018). “An Efficient Three-Field Mixed Finite Element Model for the Linear Analysis of Composite Beams with Deformable Shear Connection”. *Composite Structures*, Vol. 191, pp. 190-201.
- Foraboschi, P. (2012). “Analytical Model for Laminated-Glass Plate”. *Composites Part B: Engineering*, Vol. 43, Issue 5, pp. 2094-2106.
- Galuppi, L., Royer-Carfagni, G. (2012). “The Effective Thickness of Laminated Glass Plates”. *Journal of Mechanics of Materials and Structures*, Vol. 7, Issue 4, pp. 375-400.

-
- Galuppi, L., Manara, G., Royer-Carfagni, G. (2013). “Practical Expressions for the Design of Laminated Glass”. *Composites Part B: Engineering*, Vol. 45, Issue 1, pp. 1677-1688.
- Gjelsvik, A. (1981). “The Theory of Thin Walled Bars”. Wiley, New York.
- Gjelsvik, A. (1991). “Analog-Beam Method for Determining Shear-Lag Effects”. *Journal of Engineering Mechanics – ASCE*, Vol. 117, Issue 7, pp. 1575-1594.
- Gurtin, M.E. (1981). “An Introduction to Continuum Mechanics”. Academic Press, New York.
- Haldimann, M., Luible, A., Overend, M. (2008). “Structural Use of Glass”. *Structural Engineering Document 10*, International Association for Bridge and Structural Engineering (IABSE), Zürich.
- Hooper, J.A. (1973). “On the Bending of Architectural Laminated Glass”. *International Journal of Mechanical Sciences*, Vol. 15, Issue 4, pp. 309-323.
- Hewitt, E., Hewitt, R.E. (1979). “The Gibbs-Wilbraham Phenomenon: An Episode in Fourier Analysis”. *Archive for History of Exact Sciences*, Vol. 21, Issue 2, pp. 129-160.
- Kirchhoff, G. (1850). “Über das Gleichgewicht und die Bewegung einer elastischen Scheibe”. *Journal für die reine und angewandte Mathematik (Crelle)*, Vol. 40, pp. 51-88.
- Kirchhoff, G. (1876). “Vorlesungen über mathematische Physik – Mechanik”. Teubner, Leipzig.
- Lanczos, C. (1996). “Linear Differential Operators”. *Society for Industrial and Applied Mathematics (SIAM)*, Philadelphia.
- Lembo, M. (1989). “The Membranal and Flexural Equations of Thin Elastic Plates Deduced Exactly from the Three-Dimensional Theory”. *Meccanica*, Vol. 24, Issue 2, pp. 93-97.
- Lembo, M., Podio-Guidugli, P. (1991). “Plate Theory as an Exact Consequence of Three-Dimensional Elasticity”. *European Journal of Mechanics – A/Solids*, Vol. 10, Issue 5, pp. 485-516.
- Mindlin, R.D. (1951). “Influence of Rotary Inertia and Shear on Flexural Motions of Isotropic, Elastic Plates”. *Journal of Applied Mechanics*, Vol. 18, pp. 31-38.
- Nardinocchi, P., Podio-Guidugli, P. (1994). “The Equations of Reissner-Mindlin Plates Obtained by the Method of Internal Constraints”. *Meccanica*, Vol. 29, Issue 2, pp. 143-157.
-

-
- Newmark, N.M., Siess, C.P., Viest, I.M. (1951). “Tests and Analysis of Composite Beams with Incomplete Interaction”. *Proceedings of the Society of Experimental Stress Analysis*, Vol. 9, Issue 1, pp. 75-92.
- O’Regan, C. (2015). “Structural Use of Glass in Buildings” (2nd edition). The Institution of Structural Engineers, London.
- Podio-Guidugli, P. (1989). “An Exact Derivation of the Thin Plate Equation”. *Journal of Elasticity*, Vol. 22, Issues 2-3, pp. 121-133.
- Polya, G. (1973). “How to Solve It – A New Aspect of Mathematical Method” (2nd edition). Princeton University Press, Princeton.
- Rektorys, K. (1994). “Survey of Applicable Mathematics”, Volume 1 (2nd edition). Kluwer, Dordrecht.
- Schittich, C., Staib, G., Balkow, D., Schuler, M., Sobek, W. (2007). “Glass Construction Manual” (2nd ed.). Birkhäuser, Basel.
- Teotia, M., Soni, R.K. (2018). “Applications of Finite Element Modelling in Failure Analysis of Laminated Glass Composites: A Review”. *Engineering Failure Analysis*, Vol. 94, pp. 412-437.
- Timoshenko, S., Woinowsky-Krieger, S. (1959). “Theory of Plates and Shells” (2nd edition). McGraw-Hill, Singapore.
- Tonti, E. (1972). “On the Mathematical Structure of a Large Class of Physical Theories”. *Rendiconti della Classe di Scienze Fisiche, Matematiche e Naturali – Accademia Nazionale dei Lincei*, Serie 8, Vol. 52, pp. 48-56.
- Tonti, E. (2013). “The Mathematical Structure of Classical and Relativistic Physics – A General Classification Diagram”. Springer, New York.
- Wurm, J. (2007). “Glass Structures – Design and Construction of Self-Supporting Skins”. Birkhäuser, Basel.
-